AN INVESTIGATION OF CYLINDRICAL DETONATION WAVES

by

Benedict H. K. Lee

MERL T.N. 64-3 (GD-21)

Gasdynamics Research Laboratory
Mechanical Engineering Research Laboratories
McGill University

Montreal

March 1964

SUMMARY

A theoretical and experimental investigation of cylindrical detonation waves have been carried out.

In the theoretical phase of this investigation, the dynamics of the combustion products behind a cylindrical detonation wave is analysed by extending the Taylor-Zeldovich model of the spherical case. Based on the conservation of mass, it is shown that when the reaction zone thickness is not small compared to the radius, a steady detonation wave cannot exist. A study of the initiation mechanisms of a cylindrical detonation wave shows that it must be initially over-driven and for large radius, the Chapman-Jouguet hypothesis is satisfied.

In the experimental phase of this investigation, the detonation velocities in acetylene-oxygen mixtures with different chemical compositions (20% - 60% acetylene by volume) are determined by using ionization probes. The critical energy for spark ignition is also determined. Vertical slit streak photographs and pressure measurements are taken at different radii from the ignition source to verify that the cylindrical detonation wave is initially over-driven. Pressure measurements of the combustion products are also taken and compared with the theoretical values based on the similarity solution. The problem of transition from cylindrical deflagration to detonation, and the phenomena of spinning and pulsations are also investigated.

ACKNOWLEDGEMENTS

The Author wishes to thank Professor J.H.T. Wu for his encouragement and support.

The Author also wishes to express his gratitude to Mr. J.H.S. Lee for initiating this problem and for his advice and constructive criticisms. Thanks are due to Messrs. I. Shanfield and L.J. Vroomen for their assistance and to Miss Jeanne Rioux for her patience in typing the manuscript.

The financial assistance received from N.R.C. under Grant No. 1255 is acknowledged.

TABLE OF CONTENTS

NOMENCLATURE

Symbols

A	Constant
a	Number of moles of reactant
b	Number of moles of product
c	Speed of sound
D	Detonation velocity
E	Internal energy
E_s	Initiation energy
E_T	Total energy
ΔH	Heat of formation
h	Specific enthalpy
K	Scale factor
k	Thermal conductivity
$\vec{M}$	Momentum vector
M	Mach Number
m	Mass
n	Extent of chemical reaction that has been completed
$\vec{n}$	Unit normal vector
p	Pressure
Q	Heat of reaction per unit mass of reactants
$\vec{q}$	Velocity vector
R	Distance of cylindrical detonation wave from ignition source
$\mathcal{R}$	Universal Gas Constant
ΔR	Reaction zone thickness
r	Radius
T	Temperature
t	Time
u	Velocity component in X-direction
V	Film velocity
v	Specific volume
$\mathcal{W}$	Molecular weight
$\overline{\mathcal{W}}$	Average molecular weight of mixture
x	Similarity parameter ($^{x}/_{t}$)
y	Pressure ratio

Greek Letters

β	Concentration by weight of reactants which is free to react
γ	Ratio of specific heats
μ	Density ratio
ρ	Density
ξ, ψ, η	Non-dimensional parameters
δ_{ij}	Kronecker delta
τ_{ij}	A tensor quantity
Φ	Dissipation function
ω	Magnification factor

Subscripts

o	Unreacted state
1	Conditions at Chapman-Jouguet plane
i	ith component of the mixture
R	Conditions inside reaction zone

CHAPTER I

INTRODUCTION

The complexity of the detonation process and the experimental difficulties (a large volume of gas is required for a relatively short time under which the process can be observed) are, perhaps, the reasons for the lack of any satisfactory theory that predicts the behaviour of a detonation wave propagating into an unconfined medium. The literature on unconfined detonations is few, and the validity of the Taylor-Zeldovich model of a spherical detonation has not been critically examined. It is not surprising that this problem has received relatively little attention since plane detonation and its allied phenomena are still not fully understood yet. However, it seems that a better insight to some of the proposed postulates for plane detonations may be obtained by considering detonation waves of other geometrical configurations.

The possibilities of occurrence and propagation of unconfined detonations are not only of academic interest but are of great importance from the point of view of explosion safety. One of the early applications is the prevention of explosions in coal mines. In recent years, this question of explosion safety has become more important in connection with the design of safety devices to prevent fire hazards due to accidental spillage of liquid hydrogen and oxygen in rockets.

The cylindrical detonation wave is of special interest in the understanding of unconfined detonations since it retains the characteristics of the plane and spherical cases and yet it can be studied experimentally without any difficulties. It is believed that previous contradictions and uncertainties in unconfined detonations can be clarified by using a two-dimensional model since it facilitates better photographic observations as to the nature of stability and structure of unconfined detonation waves, the transition phenomenon and the gasdynamics of the combustion products.

CHAPTER II

DISCUSSION OF THE PROBLEM

2.1 REVIEW OF EXISTING WORK

The possibility of a spherical detonation wave having the same velocity as a plane wave was first considered by Jouguet (Reference 1) in 1906. His analysis showed that the density behind the wave front changes with time, and hence Jouguet concluded that a spherical detonation with constant speed is not possible since the wave depends on the conditions behind it. Laffitte (Reference 2) first experimented with spherical detonations in mixtures of $CS_2 + 3O_2$ and $2H_2O + O_2$, but the true nature of the waves observed was doubtful, and hence no conclusions can be drawn from his experiments.

Taylor (Reference 3) and independently Zeldovich (Reference 4) proposed a theoretical model that predicts the conditions of the gasdynamics of the burnt gas that have to be satisfied in order that a steady spherical detonation can exist. Manson and Ferrie (Reference 5) measured the velocities of spherical detonations in different fuel-oxygen mixtures and found them to agree with those of plane detonations. Hence, they concluded that the Taylor-Zeldovich theory is satisfactory. But this theory is developed based on some physically unrealistic assumptions, such as, an infinitely thin reaction zone, the existence of a rarefaction shock, and a steady wave can propagate out radially from the centre at the Chapman-Jouguet velocity. Using a spherical geometry, it is not possible to verify the Taylor-Zeldovich theory experimentally since only the wave velocity can be measured and this is the most insensitive parameter in the studies of detonation waves.

After the investigations of Taylor, Zeldovich and Manson, no further significant experimental nor theoretical work has been performed towards a better understanding of the problem of unconfined detonations. Most of the recent work done is of an experimental nature. Great effort is devoted in the study of the critical energies necessary for the initiation of detonations in different fuel-oxygen mixtures, and also the effects of additives on the formation of detonations under unconfined conditions. All these investigations are reported in References (6 to 10). The conclusions that can be drawn are: Self-sustained spherical detonation waves can be

initiated in a large variety of fuel-oxygen mixtures provided that sufficiently strong ignition sources are used, and that the limits of detonability are narrower than those for plane detonations in tubes.

The problem of transition from deflagration to detonation under unconfined conditions has not been fully understood yet. Contradictions exist among numerous investigators as to whether transition can actually occur. Chu (Reference 11) considered the problem of a spherical flame propagating into a combustible gas. He solved the hydrodynamic equations governing the flow inside the flame. He then extended Taylor's (Reference 12) solution of an expanding sphere to the flow field outside the spherical flame. The conclusion that can be drawn from this analysis is that transition under unconfined conditions is not possible since an unrealistic high rate of heat release is required. However, from the results of Manson and Ferrie (Reference 5) and Freiwald and Koch (Reference 8), pre-detonation deflagration waves were observed. The true nature of these pre-detonation deflagration waves is doubtful because their structures cannot be clearly recorded by photographic means.

2.2 OUTLINE OF THE PROBLEM

The aim of the present investigation is to further understand the problem of unconfined detonations. A two-dimensional cylindrical geometry is used since it facilitates better photographic observations. Also, the gasdynamics of the combustion products can be studied experimentally which is not possible in three-dimensional models.

The outline of the investigation is:

(a) The gasdynamics of a cylindrical detonation wave is analysed by extending the Taylor-Zeldovich model for the three-dimensional case.

(b) The distributions of fluid properties behind a cylindrical detonation wave are solved numerically on a digital computer.

(c) The rate of energy release per unit surface area of a cylindrical detonation wave is calculated.

(d) The question whether a steady cylindrical detonation wave exists is investigated.

(e) The initiation mechanisms of cylindrical detonations are discussed.

(f) The validity of the similarity solution is examined.

(g) The dynamics of the combustion products are studied experimentally by taking speed and pressure measurements.

(h) The transition phenomenon is studied experimentally by using different ignition methods. The mechanisms that promote transition are isolated and examined individually.

(i) The stability and spinning phenomena are investigated.

CHAPTER III

THEORETICAL BACKGROUND OF PLANE DETONATION WAVES

3.1 ONE-DIMENSIONAL THEORY OF STATIONARY DETONATION WAVES

A detonation wave is simply a shock wave followed by a region where chemical reaction takes place. The theory is based on the Rankine-Hugoniot equations of a shock wave which are derived from the consideration of the conservation laws of mass, momentum and energy.

Imagine that the detonation wave is confined within solid boundaries and all motions connected with the detonation take place in the direction of the x-axis, that is, the problem is considered as one-dimensional. Furthermore, it is assumed that the detonation wave has reached its stationary stage, so that its structure is independent of time, and its velocity is constant (Figure 1a). Choosing a new coordinate system that moves along with the wave front, the process can be looked upon as stationary (Figure 1b). Let the origin of the x-coordinate be at the wave front. The unburnt mixture occupies the space $x>0$. The chemical reaction starts at $x = 0$ and occurs in successive stages in the space $x<0$.

Let β be the concentration by weight of the reactants which is free to react in the given mixture, and n be the extent of the chemical reaction that has been completed. β and n are related by the expression

$$\beta = 1 - n \qquad \ldots\ldots (1)$$

and n is equal to one when the reaction is completed.

In Figure (1b), let the reaction zone be of finite thickness. Writing the conservation laws at any value of β one has,

Mass Conservation:

$$\rho_0 D = \rho (D - u) \qquad \ldots\ldots (2)$$

Momentum Conservation:

$$P_0 + \rho_0 D^2 = P + \rho (D - u)^2 \qquad \ldots\ldots (3)$$

Energy Conservation:

$$\frac{P_o}{\rho_o} + \frac{D^2}{2} + E_o = \frac{p}{\rho} + \frac{(D-U)^2}{2} + E \qquad \ldots\ldots (4)$$

Combining Equations (2) and (3) gives:

$$p - P_o = \frac{D^2}{V_o^2}(V_o - V) \qquad \ldots\ldots (5)$$

and $$U^2 = (p - p_o)(V_o - V) \qquad \ldots\ldots (6)$$

where v is the specific volume.

When Equations (5) and (6) are substituted in the energy equation, one obtains,

$$\frac{\gamma}{\gamma-1} pV + (\beta - 1)Q = (V + V_o)\frac{(p + p_o)}{2} \qquad \ldots\ldots (7)$$

where Q is the heat of reaction per unit mass of reactants.

Since p_o is small compared to p, it can be neglected. The specific volume can then be expressed as:

$$V = -\frac{V_o^2}{D^2} p + V_o \qquad \ldots\ldots (8)$$

Substituting Equation (8) into Equation (7) and after simplification yields:

$$p = \frac{D^2}{V_o(\gamma+1)}\left[1 \pm \sqrt{1 - \frac{2(\gamma^2-1)nQ}{D^2}}\right] \qquad \ldots\ldots (9)$$

and

$$V = \frac{V_o}{\gamma+1}\left[\gamma \mp \sqrt{1 - \frac{2(\gamma^2-1)nQ}{D^2}}\right] \qquad \ldots\ldots (10)$$

For different values of n, a family of Hugoniot curves can be drawn using Equations (9) and (10). The positive and negative signs in the two equations represent the intersections of the Rayleigh line $p = \frac{D^2}{v_o^2}(v_o - v)$ with the Hugoniot adiabatic of any given n.

Consider the case when reaction is completed, that is, n = 1 (Figure 2). The Rayleigh line can intersect the Hugoniot curve at three points (A, B, or C). In the next section, it is shown that only the tangent point C is permissible. Under this condition, the detonation wave velocity is,

$$D = u_1 + c_1 \qquad \ldots\ldots (11)$$

and corresponds to the minimum propagation velocity.

From Mass Conservation,

$$\frac{u_1}{D} = 1 - \frac{1}{\mu_1} \qquad \ldots\ldots (12)$$

where $\mu_1 = \frac{\rho_1}{\rho_o}$

Substituting Equations (11) and (12) into (3) gives:

$$y_1 = 1 + \frac{\rho_o D^2}{P_o}\left(1 - \frac{1}{\mu_1}\right) \qquad \ldots\ldots (13)$$

where $y_1 = \frac{P_1}{P_o}$

3.2 THE CHAPMAN-JOUGUET HYPOTHESIS

The Chapman-Jouguet hypothesis is based on the postulate that for a stable detonation wave to exist, the Rayleigh line is tangent to the Hugoniot curve. The following arguments that the intersection points A and B (Figure 2)

do not exist are based on the work of von Neumann and Zeldovich. A more detailed analysis can be found in References (13) and (4).

The variation of the fluid properties can depend on the concentration β alone. Differentiating Equations (7) and (8) with respect to β, one obtains,

$$\left\{\frac{\gamma+1}{2(\gamma-1)}v - \frac{1}{2}v_0\right\}\frac{dp}{d\beta} + \frac{\gamma+1}{2(\gamma-1)}\frac{dv}{d\beta} = 0 \qquad \ldots\ldots (14)$$

and

$$\frac{dp}{d\beta} + \frac{D^2}{v_0^2}\frac{dv}{d\beta} = 0 \qquad \ldots\ldots (15)$$

Eliminating $\frac{dp}{d\beta}$ in Equations (14) and (15), and substituting the value of p in Equation (8) give the following expression:

$$\frac{dv}{d\beta} = \frac{v_0^2(\gamma^2-1)Q}{D^2\{(\gamma+1)v - \gamma v_0\}} \qquad \ldots\ldots (16)$$

The value of β decreases from one at the wave front to zero when the reaction is completed, so that $d\beta < 0$. Due to combustion, the temperature increases and the density decreases. Therefore $dv > 0$. $\frac{dv}{d\beta}$ is then negative. Therefore $(\gamma+1)v - \gamma v_0 \leq 0$, or

$$v_0 - v \geq \frac{v}{\gamma} \qquad \ldots\ldots (17)$$

From Equation (8),

$$D^2 = \frac{p v_0^2}{v_0 - v} \qquad \ldots\ldots (18)$$

Substituting Equation (17) into (18), the following inequality holds:

$$D^2 \leq \frac{\gamma p v_0^2}{v} \qquad \ldots\ldots (19)$$

but from the mass conservation.

$$\frac{v_0}{v} = \frac{D}{D-u} \qquad \text{..... (20)}$$

and the speed of sound can be expressed as

$$c = v\sqrt{\frac{\gamma p}{v}} \qquad \text{..... (21)}$$

On combining equations (19), (20) and (21) one obtains:

$$D - u \leq c$$

or $$D \leq u + c$$

When reaction is completed, $\eta = 1$, the inequality is then

$$D \leq u_1 + c_1 \qquad \text{..... (22)}$$

For $D < u_1 + c_1$, the point of intersection of the Rayleigh line and the Hugoniot curve is at A (Figure 2). For end states that fall on this branch of the Hugoniot curve above the tangent point C, they are called strong detonations. From the consideration of the chemical process inside the reaction zone, it is seen that point B (weak detonation) is not possible. The next problem is to show that a strong detonation does not exist, and the only possible case is $D = u_1 + c_1$.

In Section 3.1, it is assumed that the combustible gas is enclosed by solid boundaries, hence it is logical to assume a back wall behind it, say Q (Figure 1b). If a moving coordinate system is chosen, the back wall must move at a velocity D in order that the boundary conditions are satisfied. The burnt gas now lies between the planes P and Q, and since they move at different velocities, they have to be connected by a rarefaction wave. P is the head of the rarefaction wave which moves at a velocity $-(D - u_1) + c_1$

Hence $-(D-u_1)+c_1 > 0$ or $D < u_1 + c_1$

implies that the rarefaction wave would enter the reaction zone (0,P) and disturb its stationarity. Therefore D must be greater than $u_1 + c_1$. But from the consideration of the reaction process inside the reaction zone (0,P), D cannot be greater than $u_1 + c_1$. The only possible solution is then $D = u_1 + c_1$ since $D \gtrless u_1 + c_1$ is not possible. This is the Chapman-Jouguet hypothesis for stable detonations.

3.3 THEORETICAL CALCULATION OF DETONATION VELOCITIES

In this section, the theoretical calculation of detonation velocities for hydrocarbon-oxygen mixtures is given. Only the non-dissociative case is considered, and a more detailed procedure can be found in Reference (14).

Consider the class of reactions:

$$a_0 C_x H_y + a_1 O_2 \longrightarrow b_1 CO_2 + b_2 H_2O + b_3 O_2 + b_4 CO \quad \ldots\ldots (23)$$

where a_i is the number of moles of the ith reactant and b_i is the number of moles of the ith product. Since a_0 is arbitrary, it can be chosen as one.

The total number of moles of each species remains constant and is expressed by the following equations:

$$\begin{aligned} x &= b_1 + b_4 \\ y &= b_2 \\ a_1 &= b_1 + \frac{b_2}{2} + b_3 + \frac{b_4}{2} \end{aligned} \quad \ldots\ldots (24)$$

where b_3 or b_4 is equal to zero depending on whether the mixture is fuel rich or oxygen rich.

For one-dimensional steady flow of a homogeneous mixture of gases, the conservation of energy is expressed by:

$$\left(\frac{1}{2}\sum_{i=0}^{1} a_i w_i\right) D^2 + \sum_{i=0}^{1} a_i h_i(T_0)$$

$$= \left(\frac{1}{2}\sum_{i=1}^{4} b_i w_i\right)(D - u_1)^2 + \sum_{i=1}^{4} b_i h_i(T_1) \qquad \ldots\ldots (25)$$

where h_i is the specific enthalpy of the ith species and w_i is the molecular weight of the ith species. D is the velocity of the unburnt mixture and $(D - u_1)$ is the velocity of the burnt mixture (see Figure 1b). Subscripts 'o' and '1' denote the unburnt and burnt gas respectively.

Since $C_x H_y + (x + \frac{1}{4}y) O_2 \longrightarrow x\, CO_2 + \frac{1}{2} y\, H_2O$,

the heat of reaction of the hydrocarbon $\Delta H_{C_xH_y}$ can be written as:

$$\Delta H_{C_xH_y} = h_{C_xH_y} + (x + \tfrac{1}{4}y) h_{O_2} - x\, h_{CO_2} - \tfrac{1}{2} y\, h_{H_2O} \qquad \ldots\ldots (26)$$

where $\Delta H_{C_xH_y} > 0$ for exothermic reaction.

Define $\Delta h_i = h_i(T_1) - h_i(T_0)$

and the heat of formation of the ith product by ΔH_i , where $i = 1, \ldots 4$.

The energy equation can be rewritten in the form:

$$\frac{1}{2}\left\{ D^2 \sum_{i=0}^{i} a_i w_i - (D-u_1)^2 \sum_{i=1}^{4} b_i w_i \right\} - b_1 \Delta h_{CO_2} - b_2 \Delta h_{H_2O}$$

$$- b_3 \Delta h_{O_2} - b_4 \Delta h_{CO} + \Delta H_{C_xH_y}(T_0) + \left(\tfrac{1}{2}y - b_2\right) \Delta H_{H_2O}(T_0)$$

$$+ (x - b_1) \Delta H_{CO_2}(T_0) - b_4 \Delta H_{CO}(T_0) + \left(a_1 - b_3 - x - \tfrac{1}{4}y\right) \Delta H_{O_2}(T_0)$$

$$= 0 \qquad \ldots\ldots (27)$$

The mass and momentum conservation laws in Section 3.1 can be arranged in a form that is useful for the calculation of the detonation velocities. Let $\overline{w}$ be the average molecular weight of the mixture and γ the ratio of the specific heats. Using the frozen sound speed, the Mach No. M_1 and M_0 can be expressed as:

$$M_1 = (D - u_1) \Big/ \left(\frac{\gamma_1 R T_1}{\overline{w}_1}\right)^{\frac{1}{2}} \qquad \ldots\ldots (28)$$

$$M_0 = D \Big/ \left(\frac{\gamma_0 R T_0}{\overline{w}_0}\right)^{\frac{1}{2}} \qquad \ldots\ldots (29)$$

where R is the Universal Gas Constant. The continuity and momentum equations can be written as:

$$\frac{D - u_1}{D} = \frac{\overline{w}_0}{\overline{w}_1} \frac{p_0}{p_1} \frac{T_1}{T_0} \qquad \ldots\ldots (30)$$

$$\frac{p_0}{p_1} = \frac{1 + \gamma_1 M_1^2}{1 + \gamma_0 M_0^2} \qquad \ldots\ldots (31)$$

For given p_0 and T_0, and an assumed value of D, there are three unknowns p_1, T_1, u_1 in the Equations (27), (30) and (31). The Newton-Raphson method is often used for the solution of these equations, and for a given set of initial data, the equations generally give two solutions that correspond to weak and strong detonations. To find the Chapman-Jouguet velocity, D is varied until the two solutions coalesce.

3.4 CONFINED PLANE DETONATION WAVES

The theoretical calculation of the Chapman-Jouguet detonation velocities is based on the assumption that the wave is plane and unconfined. In actual cases, confining boundaries are present, and precise measurements of detonation velocities have been found to be less than the theoretically predicted values. Two theories for this velocity deficit are discussed.

(1) VELOCITY DEFICIT

Fay (Reference 15) proposed a model for gaseous detonations in finite diameter tubes. The flow is viewed in a coordinate system fixed at the wave front (Figure 3), so that the tube wall has a velocity D. In this coordinate system, the wall has a velocity higher than the bulk of the gas. The velocity in the boundary layer is greater than that of the main stream, and the density is also greater because of the conduction of heat through the wall. The mass flow per unit area in the boundary layer is therefore larger than the rest of the gas stream. This can be looked upon as a negative displacement thickness which causes a gradual divergence of the stream lines.

Fay assumed a turbulent boundary layer and used an approximate expression for the boundary layer thickness based on experimental measurements. The flow in the reaction zone is steady and subsonic. It is sonic at the Chapman-Jouguet plane and becomes supersonic as the streamlines continue to diverge. For supersonic flow behind the Chapman-Jouguet plane, the Rayleigh line intersects the Hugoniot curve on the weak detonation branch of the curve, and hence the detonation velocity is less than the Chapman-Jouguet velocity.

(2) TURBULENT STRUCTURE OF GASEOUS DETONATIONS

From the interferograms of both Chapman-Jouguet and slightly overdriven detonations, White (Reference 16) observed that the flow in and behind the reaction zone is turbulent. White's analysis assumed isotropic turbulence and a mean gas velocity parallel to the axis of the tube. The transverse derivatives of any time averaged quantity vanish and the fluctuating quantities are superimposed on the time averaged velocity, pressure etc. . The Chapman-Jouguet hypothesis is modified by taking it as the minimum propagation velocity for which the conservation laws for turbulent flow are satisfied at the rear of the reaction zone. The solution of the equations for turbulent motion leads to the conclusion that the final state behind a self-sustaining detonation with turbulent reaction zone lies on the weak branch of the Hugoniot curve, and hence the detonation velocity is less than that when turbulence is absent.

(3) SOME EXPERIMENTAL OBSERVATIONS

The effect of tube diameter on the detonation velocities was carried out by Edwards et. al. (References 17 and 18) for hydrogen-oxygen mixtures initially at atmospheric pressure. Two tubes (1.6 cm and 10 cm diameter) were used, and all observed detonation velocities were lower than the calculated values. The lack of agreement was the least at the stoichiometric composition. The results obtained from the 1.6 cm diameter tube were consistently below those from the 10 cm diameter tube. The deviation from theory for $2H_2 + O_2$ mixture being -1% and -3% for the 10 cm and 1.6 cm diameter tube respectively.

Attempts were made to establish the validity of the von Neumann model. Static wall pressures and reflected pressures from the closed end of the tube were recorded by use of piezoelectric gauges. Due to the limitations of the gauges, no quantitative results of the peak pressure behind the shock were obtained, but they served to illustrate the von Neumann model qualitatively.

Pressure fluctuations were observed behind the reaction zone indicating the presence of oblique shocks. This was later confirmed from Schlieren streak photographs. The Mach number of the flow with respect to the detonation front was calculated from the average slope of the oblique shocks, and was found to be in agreement with Fay's model (Section 3.4.1).

CHAPTER IV

THEORETICAL ANALYSIS OF CYLINDRICAL DETONATION WAVES

4.1 BASIC EQUATIONS

The generalized derivation of the equations of fluid motion is given in Appendix I. They are written as:

Mass Conservation :

$$\frac{\partial \rho}{\partial t} + \nabla \cdot \rho \vec{q} = 0 \qquad \text{..... (32)}$$

Momentum Conservation :

$$\rho \frac{d\vec{q}}{dt} = \rho \vec{F} - \nabla p \qquad \text{..... (33)}$$

If the body force $\vec{F}$ is neglected and the fluid motion is symmetrical, the velocity vector $\vec{q}$ will then have only one component u. The operator ∇ is defined as:

Plane :

$$\nabla \equiv \vec{i} \frac{\partial}{\partial x} + \vec{j} \frac{\partial}{\partial y} + \vec{k} \frac{\partial}{\partial z}$$

Cylindrical :

$$\nabla \equiv \vec{r} \frac{\partial}{\partial r} + \frac{\vec{\theta}}{r} \frac{\partial}{\partial \theta} + \vec{z} \frac{\partial}{\partial z}$$

Spherical :

$$\nabla \equiv \vec{r} \frac{\partial}{\partial r} + \frac{\vec{\theta}}{r} \frac{\partial}{\partial \theta} + \frac{\vec{\Phi}}{r \sin\theta} \frac{\partial}{\partial \phi}$$

The mass and momentum conservation laws can then be written as:

$$\frac{\partial \rho}{\partial t} + \frac{\partial}{\partial r}(\rho u) + j\frac{\rho u}{r} = 0 \qquad \ldots\ldots (34)$$

and

$$\frac{\partial u}{\partial t} + u\frac{\partial u}{\partial r} + \frac{1}{\rho}\frac{\partial p}{\partial r} = 0 \qquad \ldots\ldots (35)$$

where $j = 0$ for the plane case
$j = 1$ for the cylindrical case
$j = 2$ for the spherical case

4.2 STATEMENT OF THE PROBLEM

The problem is to determine whether a steady Chapman-Jouguet cylindrical detonation wave exists or not.

Existing theories on plane detonation waves have shown that the conservation equations of mass, momentum and energy are not sufficient to determine the flow behind the detonation front. An extra condition is required and this is obtained by making the hypothesis that small disturbances in the gas immediately behind the detonation front travel at the same velocity, D, as the front itself. This condition is commonly known as the Chapman-Jouguet hypothesis and is represented by the equation $D = u_1 + c_1$, where u_1 and c_1 are the particle velocity and speed of sound of the gas immediately behind the front.

The dynamics of the burnt gas behind a detonation wave confined in a rigid tube has been solved by using Riemann's analysis (Reference 3.).

It has been shown that a progressive wave of finite amplitude behind a detonation can exist provided that the Chapman-Jouguet condition is satisfied and the conditions behind the detonation front remains constant as the detonation progresses. If a cylindrical detonation wave can be initiated instantaneously, it will satisfy the Chapman-Jouguet condition if the solution of the hydrodynamic equations for cylindrical motion satisfies the boundary condition $D = u_1 + c_1$ at a cylinder of radius $R = Dt$. The cylindrical detonation wave velocity D will be identical with that for the plane case. The fluid properties immediately behind the detonation front will be the same as those determined in Equations (12 and 13) for a plane detonation, but the radial distribution of velocity, pressure, density and temperature will be different from the plane case.

4.3 THE ASSUMPTIONS

The following assumptions for a cylindrical detonation wave are made:

(a) The fluid motion is symmetrical, and all fluid properties depend on the radius and time only.

(b) The flow is isentropic.

(c) The combustion products behave as a perfect gas with constant specific heats.

(d) A steady detonation wave is formed immediately after initiation at $r = 0$.

(e) The detonation wave propagates outwards at a constant velocity which corresponds to the Chapman-Jouguet velocity for a plane wave.

(f) The chemical reaction and transfer of mass, momentum and energy are confined in a very narrow zone which can be treated as a discontinuity.

4.4 THE SIMILARITY SOLUTION

For self-similar solutions to exist, it is necessary that the solutions in the radial coordinate at one value of time to be similar to the solutions at any other value of time. This enables a decrease in the number of independent variables from two to one, and the set of partial differential equations of fluid motion can be changed to a set of ordinary differential equations.

The gasdynamic equations for cylindrical-symmetry are:

$$\frac{\partial \rho}{\partial t} + u\frac{\partial \rho}{\partial r} + \rho\left(\frac{\partial u}{\partial r} + \frac{u}{r}\right) = 0 \qquad \ldots\ldots (36)$$

and

$$\frac{\partial u}{\partial t} + u\frac{\partial u}{\partial r} + \frac{1}{\rho}\frac{\partial p}{\partial r} = 0 \qquad \ldots\ldots (37)$$

The initial conditions at time $t=t_o$ are: $u=u_o$ and $r=r_o$.
At any other value of time, t, let $u = K_u \bar{u}$, $r = K_r \bar{r}$, $\rho = K_\rho \bar{\rho}$, $p = K_p \bar{p}$ and $t = K_t \bar{t}$, where K_u, K_r, K_p, K_ρ, and K_t are some constant scale factors and the bar quantities are for a self-preserving system.

Equations (36) and (37) can be written as:

$$\frac{K_\rho}{K_t}\frac{\partial \bar{\rho}}{\partial \bar{t}} + \frac{K_u K_\rho}{K_r}\bar{u}\frac{\partial \bar{\rho}}{\partial \bar{r}} + \frac{K_\rho K_u}{K_r}\bar{\rho}\left(\frac{\partial \bar{u}}{\partial \bar{r}} + \frac{\bar{u}}{\bar{r}}\right) = 0 \qquad \ldots\ldots (38)$$

$$\frac{K_u}{K_t}\frac{\partial \bar{u}}{\partial \bar{t}} + \frac{K_u^2}{K_r}\bar{u}\frac{\partial \bar{u}}{\partial \bar{r}} + \frac{K_p}{K_\rho K_r}\frac{1}{\bar{\rho}}\frac{\partial \bar{p}}{\partial \bar{r}} = 0 \qquad \ldots\ldots (39)$$

After simplifications, Equations (38) and (39) take the form:

$$\frac{\partial \bar{\rho}}{\partial \bar{t}} + \frac{K_u K_t}{K_r}\frac{\partial \bar{\rho}}{\partial \bar{r}} + \frac{K_u K_t}{K_r}\bar{\rho}\left(\frac{\partial \bar{u}}{\partial \bar{r}} + \frac{\bar{u}}{\bar{r}}\right) = 0 \qquad \ldots\ldots (40)$$

$$\frac{\partial \bar{u}}{\partial \bar{t}} + \frac{K_u K_t}{K_r}\bar{u}\frac{\partial \bar{u}}{\partial \bar{r}} + \frac{K_p K_t}{K_\rho K_r K_u}\frac{1}{\bar{\rho}}\frac{\partial \bar{p}}{\partial \bar{r}} = 0 \qquad \ldots\ldots (41)$$

The solutions are self similar if

$$\frac{K_u K_t}{K_r} = 1$$

and

$$\frac{K_p}{K_\rho} = 1$$

Since a perfect gas is considered, the condition that $\frac{K_p}{K_\rho} = 1$ is automatically satisfied. In order to satisfy the boundary conditions, $K_u\bar{u} = u_o$. Hence $K_u = 1$.

Therefore $\frac{K_r}{K_t}$ must be equal to unity, and the similarity parameter for this set of hydrodynamic equations is r/t.

4.5 GAS-DYNAMIC EQUATIONS FOR CYLINDRICAL DETONATION WAVES

(1) GOVERNING EQUATIONS

The fundamental equations governing the flow behind a cylindrical

detonation wave can be obtained from Equations (34) and (35) by setting $j = 1$. They are:

Mass Conservation:

$$\frac{\partial \rho}{\partial t} + u\frac{\partial \rho}{\partial r} + \rho\left(\frac{\partial u}{\partial r} + \frac{u}{r}\right) = 0$$

Momentum Conservation:

$$\frac{\partial u}{\partial t} + u\frac{\partial u}{\partial r} + \frac{1}{\rho}\frac{\partial p}{\partial r} = 0$$

Using the similarity parameter derived in Section 4.4, and define it as $x = \frac{r}{t}$, then the mass and momentum conservation laws can be combined to give the following equation:

$$\frac{du}{dx}\left\{1 - \left(\frac{x-u}{c}\right)^2\right\} = -\frac{u}{x} \qquad \ldots\ldots (42)$$

The mass and momentum conservation laws can also be expressed in a non-dimensional form by defining $\xi = u/x$, $\eta = c^2/x^2$ and $Z = \ln x$. The resulting equations are:

$$\frac{dZ}{d\xi} = -\frac{1}{\xi}\left\{\frac{\eta - (1-\xi)^2}{2\eta - (1-\xi)^2}\right\} \qquad \ldots\ldots (43)$$

and

$$\frac{d\eta}{d\xi} = \frac{\eta}{\xi}\left\{\frac{2\eta - 2(1-\xi)^2 + f\xi(1-\xi)}{2\eta - (1-\xi)^2}\right\} \qquad \ldots\ldots (44)$$

where

$$f = \gamma - 1$$

Equations (43) and (44) are further transformed so that they can be used in a computer. Define $\psi = \frac{u}{c}$ so that $\eta = \xi^2/\psi^2$, the two equations can be written as:

$$\frac{d\xi}{dZ} = \xi \left\{ \frac{2\xi^2 - (1-\xi)^2\psi^2}{(1-\xi)^2\psi^2 - \xi^2} \right\} \qquad \ldots\ldots (45)$$

$$\frac{d\psi}{dZ} = \frac{\xi\psi}{2} \left\{ \frac{2\xi - (1-\xi)\xi\psi^2}{(1-\xi)^2\psi^2 - \xi^2} \right\} \qquad \ldots\ldots (46)$$

The complete derivation of Equations (45) and (46) is given in Appendix II.

The radius of the detonation wave at any instant of time t is R = Dt where D is the wave velocity. Therefore, x = D (r/R), and since only increments of Z are considered in equations (45) and (46), one can write Z = ln (r/R). From the expressions $\xi = \frac{u}{x}$ and $\psi = \frac{u}{c}$, the particle velocity and speed of sound can be written as:

$$\frac{u}{D} = \xi \left(\frac{r}{R}\right) \qquad \ldots\ldots (47)$$

and

$$\frac{c}{D} = \frac{\xi}{\psi} \left(\frac{r}{R}\right) \qquad \ldots\ldots (48)$$

(2) BOUNDARY CONDITIONS:

The boundary conditions that have to be satisfied are:

(a) Zero velocity at the centre (i.e. u = 0 at r = 0), and

(b) The detonation wave velocity is constant and corresponds to that for a Chapman-Jouguet plane detonation.

Under condition (b), the following equations from Chapter III must hold immediately behind the wave front. They are:

$$D = u_1 + c_1$$

$$\frac{u_1}{D} = 1 - \frac{1}{\mu_1}$$

$$y_1 = 1 + \frac{\rho_0 D^2}{P_0}\left(1 - \frac{1}{\mu_1}\right)$$

The values of ξ and ψ at the wave front (i.e. r = R) that have to satisfy Equations (47) and (48) are:

$$\xi_1 = 1 - \frac{1}{\mu_1} \qquad \ldots\ldots (49)$$

and

$$\psi_1 = \mu_1 - 1 \qquad \ldots\ldots (50)$$

(3) FLUID PROPERTIES OF THE PRODUCTS OF COMBUSTION

From Equation (48), since $\frac{c_1}{D} = \frac{\xi_1}{\psi_1}$, the speed of sound ratio $\frac{c}{c_1} = \frac{\xi\psi_1}{\xi_1\psi}\left(\frac{r}{R}\right)$. The pressure, density and temperature when expressed in terms of ξ, ψ and $\left(\frac{r}{R}\right)$ are:

Pressure Ratio

$$\frac{P}{P_1} = \left(\frac{c}{c_1}\right)^{2\gamma/\gamma-1} = \left\{\frac{\xi\psi_1}{\xi_1\psi}\left(\frac{r}{R}\right)\right\}^{2\gamma/\gamma-1} \qquad \ldots\ldots (51)$$

or

$$\frac{P}{P_0} = \left\{1 + \frac{\rho_0 D^2}{P_0}\left(1 - \frac{1}{\mu_1}\right)\right\}\left\{\frac{\xi\psi_1}{\xi_1\psi}\left(\frac{r}{R}\right)\right\}^{2\gamma/\gamma-1} \qquad \ldots\ldots (52)$$

Density Ratio

$$\frac{\rho}{\rho_1} = \left(\frac{c}{c_1}\right)^{2/\gamma-1} = \left\{\frac{\xi\psi_1}{\xi_1\psi}\left(\frac{r}{R}\right)\right\}^{2/\gamma-1} \qquad \ldots\ldots (53)$$

or

$$\frac{\rho}{\rho_0} = \mu_1 \left\{ \frac{\xi \psi_1}{\xi_1 \psi} \left(\frac{r}{R} \right) \right\}^{2/\gamma - 1} \qquad \ldots\ldots (54)$$

Temperature Ratio

$$\frac{T}{T_1} = \left(\frac{c}{c_1} \right)^2 = \left\{ \frac{\xi \psi_1}{\xi_1 \psi} \left(\frac{r}{R} \right) \right\}^2 \qquad \ldots\ldots (55)$$

or $$\frac{T}{T_0} = \frac{1}{\mu_1} \left\{ 1 + \frac{\rho_0 D^2}{P_0} \left(1 - \frac{1}{\mu_1} \right) \right\} \left\{ \frac{\xi \psi_1}{\xi_1 \psi} \left(\frac{r}{R} \right) \right\}^2 \qquad \ldots\ldots (56)$$

4.6 NUMERICAL SOLUTION OF THE GASDYNAMIC EQUATIONS FOR CYLINDRICAL DETONATION WAVES

In the numerical solution, the values of the specific heats ratio (γ) and the density ratio (μ_1) for $C_2H_2 + O_2$ mixture are taken as 1.13 and 1.87 respectively. These values have taken into account the dissociation and variation in specific heats at the temperature of the detonation front, and are obtained from Reference (19). Using $\gamma = 1.13$, and $\mu_1 = 1.87$, the values of ξ and ψ at the wave front are: $\xi_1 = 0.465$ and $\psi_1 = 0.870$.

On examining Equations (45) and (46), $d\xi/dZ$ and $d\psi/dZ$ are infinite at the wave front ($r = R$) since the denominator $(1-\xi)^2\psi^2 - \xi^2$ is equal to zero when $\xi_1 = 1 - \frac{1}{\mu_1}$ and $\psi_1 = \mu_1 - 1$.

In order to find a solution, it was necessary to work backwards from the wave front. ξ_1 and ψ_1 were taken to be 0.465 and 0.870 respectively when $\frac{r}{R} = 0.9999$. Equations (45) and (46) where programmed on the IBM 1410 digital computer, and the Runge-Kutta method was used to find ξ and ψ for different values of r/R. The interval ΔZ was taken to be 0.0001.

Equations (47), (48), (51), (53) and (55) were also computed as functions of $\frac{r}{R}$ and the solutions are given in Table I and Figures (4 and 5). The particle velocities for the plane and spherical cases are plotted in Figure (4) for comparison purposes. A brief description of the Runge-Kutta method is given in Appendix III.

4.7 INITIATION OF CYLINDRICAL DETONATIONS

For the initiation of unconfined detonations, sufficiently large energies (approximately 10 joules) are required (References 6 to 10). Unlike the plane case, unconfined detonations have to be initiated instantaneously within a very short induction time since transitions from deflagrations to detonations are not possible.

In Chapter III, a detonation has been considered as a shock wave followed by a region where chemical reaction occurs. The reaction takes place in the gas compressed by the shock wave and the thickness of the reaction zone depends on the rate of reaction. It is thus logical to relate the initiation mechanisms of a detonation wave by considering the propagation of a strong shock or blast wave in a reactive mixture.

The instantaneous release of energy from the ignition source generates a strong blast wave which decays rapidly as it propagates into the reactive mixture. The criterion for instantaneous initiation of a detonation by the blast wave is that the time taken for the high pressure behind the blast wave to decay to the Chapman-Jouguet pressure must be larger than the induction time. This is similar to the role played by the shock in a detonation wave where the reactants are compressed to a high temperature and pressure so that auto-ignition occurs and reaction is completed in a thin region behind the shock front. For a weak blast wave, the time taken for the wave to decay from a high pressure to the Chapman-Jouguet pressure is shorter than the induction time. A deflagration wave results since transition to detonation under unconfined conditions is not possible.

Denoting the region where chemical reaction is completed as the reaction zone thickness, the pressure at the end of reaction depends initially on the strength of the blast wave since the chemical energy released is small compared to the ignition energy. The large energy required overdrives the detonation at its early stages. Since the reaction zone thickness depends on the strength of the preceeding shock (a stronger shock

compresses the reactive mixture more and hence a shorter reaction time), it will become larger as the wave decays until at large radius, it is constant and equivalent to that for a plane detonation. The fact that the reaction zone thickness is thinner for an overdriven detonation as compared to that for self-sustained detonation can be observed from the interferograms of White (Reference 16).

It is possible to predict the behaviour of a cylindrical detonation wave qualitatively by a consideration of the energy enclosed inside the wave. Let E_s be the initiation energy and at any instant of time the wave has travelled a distance R from the centre. Assuming that the chemical energy inside the reaction zone is completely liberated, the total energy is therefore;

$$E_T = E_s + \pi R^2 \rho_o Q \qquad \ldots\ldots (57)$$

where Q is the chemical energy per unit mass of the reactive mixture.

For very small radius R, the chemical energy is small compared to the initiation energy and can be neglected. The detonation wave is essentially a blast wave and according to Lin's (Reference 21) analysis of a cylindrical blast, the pressure behind the wave front decays inversely proportional to the square of the radius.

When the radius is large, then $\pi R^2 \rho_o Q \gg E_s$. The pressure behind the detonation wave is constant and corresponds to that behind a plane detonation. This can be seen from Eqns. (4.), (8), (9) and (10) in Section 3.1 that the pressure (p_1) behind the front wave is:

$$p_1 = A Q \rho_o \qquad \ldots\ldots (58)$$

where A is a proportionality factor. The pressure is constant since for a given reactive mixture, the chemical energy Q and the initial density ρ_o are constant.

It is not possible to predict how does the pressure decay when the initiation energy and the chemical energy are of the same order of magnitude. Since there can be no pressure discontinuities in this region, a well behaved curve is suspected. This will be verified later by measuring the pressures experimentally.

Summarizing, the following model of initiation of a cylindrical detonation wave is proposed: A sufficiently large energy is required to generate a blast wave so that the time taken for the high pressure behind the blast to decay to the Chapman-Jouguet pressure is greater than the induction time. For small radius, the pressure decays inversely proportional to the square of the radius, and for large radius, it corresponds to that for a plane Chapman-Jouguet detonation.

4.8 THE ENERGY LAW

Let E_s be the energy required to initiate a cylindrical detonation wave, and Q the heat of reaction per unit mass. Consider the wave to be of unit thickness, then the total energy at any time will be

$$E_T = E_s + \int_0^R 2\pi r \rho Q \, dr \qquad \ldots\ldots (59)$$

The integral

$$\int_0^R 2\pi r \rho Q \, dr = 2\pi Q \rho_0 \int_0^R \frac{\rho}{\rho_0} r \, dr$$

From Equation (54),

$$\frac{\rho}{\rho_0} = \mu_1 \left\{ \frac{\xi \psi_1}{\xi_1 \psi} \left(\frac{r}{R} \right) \right\}^{2/\gamma - 1}$$

Therefore,

$$\int_0^R 2\pi r \rho Q \, dr = 2\pi Q \rho_0 \mu_1 \int_0^R \left\{ \frac{\xi \psi_1}{\xi_1 \psi} \left(\frac{r}{R} \right) \right\}^{2/\gamma - 1} r \, dr$$

By changing dr to $d\left(\frac{r}{R}\right)$, and the limits of integration from 0 to 1 instead of from 0 to R, the integral

$$\int_0^R 2\pi r \rho Q \, dr = 2\pi R^2 Q \rho_0 \mu_1 \alpha \qquad \ldots\ldots (60)$$

where

$$\alpha = \int_0^1 \left\{\frac{\xi \psi_1}{\xi_1 \psi}\right\}^{2/\gamma-1} \left(\frac{r}{R}\right)^{\frac{\gamma+1}{\gamma-1}} d\left(\frac{r}{R}\right) \qquad \ldots\ldots (61)$$

Since $\frac{r}{R}$ varies from 0 to 1, and the values of ξ and ψ as functions of $\frac{r}{R}$ are known, the value of α can be found by numerical integration of Equation (61). The integration was carried out on the IBM 1410 digital computer, and Simpson's Rule was used. The value of α was found to be 0.266.

The total energy at any time is:

$$E_T = E_s + 2\pi R^2 (0.266 Q \rho_0 \mu_1)$$

and differentiating E_T with respect to time one obtains:

$$\frac{dE_T}{dt} = 2\pi (0.266 Q \rho_0 \mu_1) 2R \frac{dR}{dt}$$

$$= 2\pi R (0.532 \rho_0 \mu_1 Q) D \qquad \ldots\ldots (62)$$

The rate of energy released from chemical reaction per unit surface area of the wave is $0.532 \rho_0 \mu_1 Q D$, and is a constant. This shows that a self-sustained cylindrical detonation wave can propagate with a constant velocity and satisfies the Chapman-Jouguet hypothesis.

CHAPTER V

NON-EXISTENCE OF STEADY CHAPMAN-JOUGUET CYLINDRICAL DETONATION WAVES

5.1 DISCUSSION OF THE GASDYNAMIC EQUATIONS FOR CYLINDRICAL DETONATION WAVES

In Chapter IV, Section 4.5, it is found that when the values of ξ_1 and ψ_1 at the wave front are subsituted into Equation (45) that is,

$$\frac{d\xi}{dZ} = \xi\left\{\frac{2\xi^2 - (1-\xi)^2\psi^2}{(1-\xi)^2\psi^2 - \xi^2}\right\}$$

the denominator is equal to zero so that $\frac{d\xi}{dZ}$ evaluated at the wave front is infinite.

But $$\frac{d\xi}{dZ} = \frac{d(U/x)}{d\ln x} = \frac{du}{dx} - \frac{U}{x} \qquad \ldots\ldots (63)$$

and at the wave front x=D, and $\frac{u}{D}$ is finite. Therefore,

$$\left.\frac{du}{dx}\right|_{r=R} = \infty \qquad \ldots\ldots(64)$$

From Equation (42),

$$\frac{du}{dx}\left\{1 - \left(\frac{X-u}{c}\right)^2\right\} = -\frac{U}{x}$$

At the wave front, $\frac{du}{dx}$ is infinite, and the relation $\left\{1 - \left(\frac{D-u_1}{c_1}\right)^2\right\} = 0$ is obtained. This simply means $D = u_1 + c_1$. Thus, it is observed that the unrealistic infinite slope of the velocity, pressure etc., is not a consequence of the similarity solution, but due to the assumption $D = u_1 + c_1$, which is initially imposed as a boundary condition in order that the hydrodynamic equations can be solved.

At large time, the detonation wave radius (Dt) tends to infinity, and the plane detonation is approached. The derivations of the fluid properties are finite, and from Equation (42),

$$\frac{du}{dx} = \frac{-u/x}{1-\left(\frac{x-u}{c}\right)^2}$$

From the computed solution of the particle velocity, it is seen that $\frac{du}{dx}$ is positive. In order for $\frac{du}{dx}$ to be finite and positive, $1-\left(\frac{x-u}{c}\right)^2$ evaluated at the wave front must be less than zero, but greater than $-\infty$. Hence it is seen that $D \geq u_1 + c_1$.

This analysis shows that $D = u_1 + c_1$ is not possible, and in order not to violate any physical law, the detonation wave must either be over - or under-driven. A study of the initiation mechanisms in Section 4.7 shows that a large energy has to be supplied to generate a blast wave. Initially, the pressure drops inversely proportional to the square of the radius and at large radius it is equal to the Chapman-Jouguet pressure. In other words, the detonation wave has to be initially overdriven and therefore $D < u_1 + c_1$.

5.2 THE MASS CONSERVATION APPROACH

It has been shown that a cylindrical detonation wave cannot propagate at a velocity $D = u_1 + c_1$. The next problem is to determine whether it is possible for a steady detonation wave to propagate outwards from the centre at the instant when it is initiated.

In Figure (7), consider at time equal to zero, a detonation wave is formed at the centre having a reaction zone of finite thickness ΔR.

Let ρ_R be the average density inside the reaction zone. For a steady wave, ΔR, ρ_R, D, u_1 and ρ_1 are independent of time.

At any time t, the wave traversed a distance R = Dt.

The mass engulfed by the wave front

$$= \pi \rho_0 \left\{ (Dt + \Delta R)^2 - (\Delta R)^2 \right\}$$

The mass in the reaction zone

$$= \pi \rho_R \left\{ (Dt + \Delta R)^2 - (Dt)^2 \right\}$$

The initial mass

$$= \pi \rho_R (\Delta R)^2$$

From the mass conservation,

Mass engulfed by the wave front + initial mass = mass in the reaction zone + mass behind the reaction zone (m_c).

Therefore,

$$m_c = \pi \rho_0 \left\{ (Dt + \Delta R)^2 - (\Delta R)^2 \right\} + \pi \rho_R (\Delta R)^2 - \pi \rho_R \left\{ (Dt + \Delta R)^2 - (Dt)^2 \right\}$$

After simplification

$$m_c = \pi \left\{ \rho_0 Dt (Dt + 2\Delta R) - \rho_R (2Dt\Delta R) \right\} \quad \ldots\ldots (65)$$

and

$$\frac{dm_c}{dt} = \pi \rho_0 \left\{ 2D^2 t + 2\Delta R D \right\} - \pi \rho_R (2D\Delta R) \quad \ldots\ldots (66)$$

For a steady wave, the mass flux across the plane where reaction is completed is

$$2\pi Dt \rho_1 (D - u_1) \quad \ldots\ldots (67)$$

Since mass is conserved, one can write:

$$\frac{dm_c}{dt} = 2\pi \rho_1 Dt\,(D - u_1)$$

or

$$2\pi \rho_0 D\,(Dt + \Delta R) - 2\pi \rho_R D \Delta R = 2\pi \rho_1 Dt\,(D - u_1)$$

Simplifying, one obtains the equation

$$\frac{\rho_1 (D - u_1) - \rho_0 D}{D(\rho_0 - \rho_R)} = \frac{\Delta R}{Dt} = \frac{\Delta R}{R} \qquad \ldots\ldots (68)$$

The right hand side of Equation (68) depends on time. The assumption that the velocities and densities are time independent are violated unless R is so large that $\frac{\Delta R}{R}$ is equal to zero. Thus, for small times t, $\frac{\Delta R}{Dt}$ is finite and cannot be neglected. Under such circumstances, a steady wave propagating outwards is not possible.

CHAPTER VI

EXPERIMENTAL INVESTIGATION

6.1 APPARATUS

For the experimental investigation of the various phenomena in cylindrical detonations, a pill box of 50 cm diameter and of adjustable width was used. The front plate of the pill box was transparent to enable photographic observations. A 1-1/2" thick plexi-glass was found to be most suitable for this purpose. Four (three 1" thick and one 1/2" thick) steel rings with inside diameter of 50 cm and outside diameter of 60 cm were bolted together and sealed by 'O' rings to give a pill box 3-1/2" wide. Different combinations of the four steel rings gave different widths. The minimum width being 1/2" and the maximum 3-1/2", in increments of 1/2". The back plate of the pill box was made of a 1/2" thick steel plate. A 3/8" diameter hole was drilled and tapped for the installation of an ignitor. Holes were also drilled in the plate for installation of ionization probes and pressure transducers. A sketch of the pill box is shown in Figure (8). The main controls for the cylindrical detonation experiments are shown in Figure (9). Commercial acetylene and oxygen were used without further purification. Mixtures of acetylene and oxygen were prepared in a 100-litre tank, and the compositions were determined by the partial pressures of the individual gas. To ensure the mixture was homogenous, a steam coil inside the 100-litre tank was used to induce a natural convection current, and hence promote better mixing.

The ignitor was designed so that it could be used for different methods of ignition. A schematic diagram of it is shown in Figure (10). For ignition by exploding wire, a .001" diameter copper wire was soldered across AB. A variable D.C. power supply (0 - 4 KV) and a variable capacitor bank (0.5 - 30 μf) were used. Different energies required to explode the copper wire could be obtained within an accuracy of $\pm$ 0.01 joules. The electrical leads were carefully selected to reduce the resistance and inductance of the circuit to a minimum. For spark ignition, a high voltage was applied across AB, and the spark gap could be adjusted by moving the central electrode. Ignition by hot wire was carried out by use of a 0.1 mm diameter Ni - Cr resistance wire heated to white hot in less than 1 second by a 36 Volts D.C. power supply.

6.2 INSTRUMENTATION

(1) IONIZATION PROBES

Figure (11) shows the details of the ionization probe used. It consisted of two steel needles placed in a ceramic insulator and spaced 2mm apart. The associated probe circuit is shown in Figure (12). The 0.005μ f capacitor was charged to a potential of 200 V through a 22 M ohms charging resistor. Initially the probe was open-circuited, but as soon as the detonation wave traversed it, the ionized gas behind the wave front completed the circuit, and the capacitor discharged through a 47K ohm resistor. The pulse obtained was displayed on an oscilloscope screen.

(2) PHOTO-TUBES

The highly luminous detonation front will cause photo-emission in a photo-sensitive element. The photo-tube circuit was designed to give a fast-response and decay pulse. The 3$\mu\mu$f capacitor was initially charged to 200V and discharged through the 1 K ohms resistor as soon as photo-emission took place, thus displaying a pulse on the oscilloscope screen. Two slits, 6" apart were placed in front of the photo-tube to ensure that no photo-emission would occur when the detonation wave was not directly in front of it. RCA 929 tubes were used and the circuit is shown in Figure (13). Independent units were built and as many of them could be used at the same time as desired.

(3) STREAK CAMERA

A high speed 35 mm rotating drum camera was designed and constructed for detonation wave studies. The outer rim of the 3.9" aluminum drum had fifteen milled buckets of the simple Pelton wheel design, and compressed air at 30 psig was used to drive the drum. The camera had a maximum speed of 15,000 rpm. A schematic diagram of the camera is shown in Figure (14).

In figure (15), an illustration of a typical streak photograph of a cylindrical detonation is shown. Let

V = Peripheral velocity of the film

D = Detonation wave velocity

α = Angle between detonation wave and film velocity vector

ω = Magnification factor = $\frac{\text{Length recorded on film}}{\text{Actual length}}$

then the detonation wave velocity is given by the equation

$$D = \frac{V \tan \alpha}{\omega} \qquad \ldots\ldots (69)$$

CHAPTER VII

RESULTS AND DISCUSSIONS

7.1 VELOCITY MEASUREMENTS

Ionization probes, photo-tubes and streak camera were used to determine the detonation velocities experimentally. The accuracy of each device is discussed below.

(1) ACCURACIES OF SPEED MEASUREMENT DEVICES

The ionization probes used had a rise time of 1.5 μ seconds. They were installed on the back plate of the cylindrical vessel. The distance between each probe was 2 cm and there was a possible alignment error of $\pm$ 0.1 mm (or $\pm$ 0.5%).

Photo-tubes with a rise time of 2 μ seconds were placed in front of the transparent plate of the cylindrical vessel. Each photo-tube had a 2 mm wide slit in front of it and the maximum error was $\pm$ 10% when they were spaced 2 cm apart.

Using the camera described in Section 6.2, the streak recorded on the film was approximately 30° to the horizontal (Figures 17 and 18). A difference of $\pm$ 1/4 ° in the measurement of the angle corresponded to an error of $\pm$ 2% in the evaluation of tan α in Equation (69). The speed of the camera was recorded from an oscilloscope and there was an uncertainty of $\pm$ 5%. The total expected error of the streak camera was $\pm$ 7%.

(2) RESULTS FROM IONIZATION PROBES

In view of the fact that ionization probes gave the most accurate results, they were used to measure the cylindrical detonation wave velocities of oxygen-acetylene mixtures with different chemical compositions (20% - 60% acetylene by volume). The initial temperature and pressure of the mixtures were kept at 300° K and 100 mm Hg respectively. The results are shown in Table II and in Figure (19), and the velocities of plane detonations confined in a one inch diameter tube are also included. They are consistently below Bollinger's (Reference 22) theoretical cal-

culations of the Chapman-Jouguet plane detonation velocities which were based on an initial pressure and temperature of 1 atmosphere and 313° K respectively. The deviations in velocities are expected since a decrease in the initial pressure results in a decrease in velocity because of the increased dissociation of the combustion products. The difference in velocity at different initial pressures have not been calculated for an acetylene-oxygen mixture. To show an idea of the dependence of velocity on initial pressure, consider the case of hydrogen-oxygen ($H_2 + O_2$) detonations. There is a difference of as much as 130 metres/second between 0.1 and 1 atmosphere initial pressure at 298° K (Reference 23).

In Section 4.7, it has been shown that a cylindrical detonation wave is initially overdriven and decays to a plane detonation at large radius from the ignition source. An attempt had been made to measure the velocities at small radii from the centre, and it was found that within the experimental error of $\pm$ 0.5%, the small change in velocity observed was not reliable. A typical oscillogram is shown in Figure (20), and it can be seen that the time taken for the detonation wave to traverse each probe is nearly constant. Similarly, streak photographs have not been able to detect any change in velocity at all (Figures 17 and 18).

On examination of the Hugoniot curve (Figure 2), it is seen that the Chapman-Jouguet state is at the point of tangency of a line drawn through the initial state tangent to the equilibrium Hugoniot. Therefore, relatively large changes in the location of the Chapman-Jouguet point on the equilibrium Hugoniot make only second order changes in the detonation velocity because the velocity is directly related to the square root of the negative slope of the line between the Chapman-Jouguet state and the initial state. This is readily seen from Equation (5) in Section 3.1. In determining the states in the equilibrium Hugoniot near the Chapman-Jouguet state, more sensitive parameters such as the pressure have to be used.

7.2 PRESSURE MEASUREMENTS

In the study of the ignition mechanisms (Section 4.7), it has been pointed out that in the region where the initiation energy and the chemical energy are of the same order of magnitude, the behaviour of the pressure cannot be predicted theoretically. It is suspected that the pressure decay is well behaved and attempts to verify this by velocity measurements have proved to be unsuccessful. It is not surprising to know why the velocity hardly changes in this region since it lies on the equilibrium Hugoniot close to the Chapman-Jouguet state (Figure 2). The velocity depends on the slope of the Rayleigh line which hardly changes at all. However, there is quite a significant change in pressure corresponding to a small change in the slope of the Rayleigh line.

A Kistler Model 603 pressure transducer was used to measure pressures near the ignition source. The transducer was calibrated in a one inch diameter detonation tube. 50% - 50% acetylene-oxygen mixtures were used and the reactive mixtures were detonated at different initial pressures. The peak voltage output from the transducer was recorded from a Tektronix 555 Oscilloscope. The corresponding pressure was calculated based on a theoretical pressure rise of 54.5 (Reference 19). A calibration curve up to a pressure of 320 psi is shown in Figure (22).

Due to the difficulties in mounting the pressure transducers on the back plate of the cylindrical vessel, it was not possible to take measurements at radii less than 2 cm from the ignition source. Within this 2 cm radius, another transducer (Atlantic Research Corporation Model BD-25) was installed for triggering the beam on the oscilloscope. The pressure measurements for radii greater than 2 cm are shown in Figure (23). 50%-50% acetylene-oxygen mixtures are used at an initial temperature and pressure of 300° K and 200 mm Hg respectively. The pressure decay is a smooth curve and at approximately 5 or 6 cm from the centre, it remains constant at a pressure of 211 psi which is exactly the same as the Chapman-Jouguet pressure. It is not possible from the experimental results to determine exactly the region where the initiation energy and the chemical energy are

of the same order of magnitude. Besides, this region changes for different initiation energies. But it can be said that the pressure decays in a well behaved manner in this region. The results also show that the detonation wave is initially over-driven and decays to a Chapman-Jouguet detonation in less than 25% the diameter of the cylindrical vessel.

At radii greater than 6 cm from the centre, it is seen that the Chapman-Jouguet condition is satisfied across the cylindrical detonation wave. The similarity solution in Section 4.4 requires that the distributions of the fluid properties of the burnt gas have similar profiles at any instant of time. Pressure measurements of the burnt gas have been taken and compared with the theoretical values based on the similarity solution.

Four Atlantic Research Corporation Model BD-25 pressure transducers were mounted on the back plate of the cylindrical vessel. The transducers mounted at 5 cm and 9 cm from the ignition source were used to trigger the beams on the oscilloscope while the two transducers at 8 and 12 cm from the centre were used to register the pressures of the burnt gas. Again, 50%-50% acetylene-oxygen mixtures at an initial temperature and pressure of 300° K and 200 mm Hg were used. A typical pressure record is shown in Figure (20). The transducers were calibrated and found to be linear within the range of 0-350 psi.

The pressure at any instant of time was non-dimensionalized with respect to the peak pressure. Figures (24) and (25) show the experimental values of the pressures of the burnt gas at different times at 8 and 12 cm from the ignition source, and the results are tabulated in Table III. The experimental errors are also shown, and the results were obtained from twenty different runs. In Figure (26), the pressures from Figures (24) and (25) are replotted as a function of (r/R). The results indicate that the pressure profiles are similar and the analysis in Section 4.5 does predict the dynamics of the combustion products quite satisfactory at sufficiently large radius from the ignition source where the Chapman-Jouguet hypothesis is satisfied.

On examining Figure (26), it is noted that the deviations of the pressure measurements from the theoretical values are greatest when $^{r}/_{R}$ is between 0.5 and 0.7. This may be due to the boundary layers developed on the two confining side plates of the cylindrical vessel or it may due to the existence of weak compression waves trailing behind the detonation front. At this stage, it is not possible to explain the peculiarity of the pressures recorded in this region until further investigations are made. Schlieren streak photographs of the detonation wave will reveal the possibility of any weak compression waves. For $^{r}/_{R}$ less than 0.3 the pressures drop below the theoretical value of 0.32, and this is due to the heat loss through the metal side plate of the cylindrical vessel.

7.3 VERTICAL SLIT STREAK PHOTOGRAPHS

In taking vertical slit streak photographs, the transparent front plate of the cylindrical vessel was covered with black tape except for a slit (1mm wide and 2 cm long) perpendicular to the vertical axis of the front plate (Figure 16). The detonation wave and the film both moved in the same direction. The effects of film speed and slit width are discussed below with special reference to Figure (27).

Case (a): Film moves with the same velocity as the wave

If the film moves at the same velocity as the wave, the trace recorded on the film represents the true thickness of the reaction zone. The width of the slit is unimportant since the result is the same with or without the presence of the slit.

Case (b): Film is stationary

The trace recorded on a stationary film is the width of the slit itself. If the reaction zone is exactly the width of the slit, the true thickness of the reaction zone is recorded.

Case (c): Film moves faster than the wave

If the film moves faster than the wave, then during the time the reaction zone takes to traverse the width of the slit, the film has moved a distance greater than the reaction zone thickness. This is true

for the three cases where the slit width is greater, less or equal to the reaction zone.

Case (d): Film moves slower than the wave

If the slit is wider or equal to the reaction zone, then the trace recorded is always greater than the reaction zone thickness. However, if the slit is slightly or very much smaller than the reaction zone, the trace can be greater or less than the reaction zone thickness.

(1) EXPERIMENTAL ERRORS

A camera speed of 220 cycles/second corresponds to a film velocity of 67.5 metres/second. On the time axis of the film, 1mm is equivalent to 0.148 μ second. An uncertainty of ± 5% in the film velocity is therefore equal to an error of ± 2.1% on the film. The slit may not be truly 1mm wide and there is a possible error of ± 0.05 mm. As the reaction zone thickness decreases, this error becomes more severe. Taking the case where the reaction zone thickness to be 1mm and the detonation velocity to be 2820 mètres/sec the error on the film is ± 2.82%.

Other errors such as the slit not being truly perpendicular to the vertical axis, the effect of the thickness of the front plate of the cylindrical vessel, three-dimensional effects near the ignition source etc., are either very small or cannot be estimated. The major errors that can be calculated are those due to the film velocity and the slit width, and they contribute a total error of approximately ± 5% of the thickness of the trace recorded on the film.

(2) INTERPRETATION OF THE RESULTS

The luminous trace recorded on a vertical streak photograph cannot be interpretated as the true reaction zone thickness. It can only be taken as a qualitative comparison of the reaction zone thickness of detonation waves under the same initial conditions.

Figure (28) shows the vertical slit streak photographs of a cylindrical detonation wave taken at different radii from the ignition

source. 50%-50% acetylene-oxygen mixtures were used at an initial temperature and pressure of 300° K and 50 mm Hg respectively. At 1 cm from the ignition source, the streak is not well defined as it is too close to the spark discharge. At 2 and 3 cm, it can be seen that the streak thickness increases, and from 4 cm onwards, it remains constant. The thickness of the streak for cylindrical and plane detonations are compared in Figure (29). For the plane detonation, the streak is constant at 3 and 20 cm from the ignition source and equals to the cylindrical case at 20 cm, but greater than that at 3 cm.

The thickness of the streak at different radii for the cylindrical detonation is divided by that for a plane detonation. Denoting this ratio by α, it is plotted as a function of radius in Figure (23). The results show that at small radius, the cylindrical detonation wave is overdriven and the reaction zone is thinner (hence a thinner streak) than that for a Chapman-Jouguet plane detonation. As the radius increases, α also increases until at approximately 4 cm from the ignition source, it is equal to one. In other words, the reaction zone thickness is the same as that for a plane detonation. The results agree very well with the pressure measurements in Section 7.2 and confirm the ignition mechanisms proposed in Section 4.7.

7.4 SYMMETRICAL WAVE SHAPE

In Chapter IV, it is assumed that the detonation wave is perfectly symmetrical. In order to justify this assumption, the instantaneous wave shapes were determined for 50%-50% acetylene-oxygen mixture at an initial pressure of 100 mm Hg. Ionization probes were installed at different radii from the ignition source. The solid lines in Figure (30) are the theoretical wave shapes at different times after ignition. The theoretical values are based on a detonation velocity of 2820 metres/second. Within the $\pm$.5% accuracy of the ionization probes, it can be said that the cylindrical detonation wave is perfectly symmetrical about the centre.

7.5 THE TRANSITION PHENOMENON

The problem of transition from deflagration to detonation in constant area ducts has in recent years been critically studied (References 24 to 28). Unfortunately, the problem is extremely complicated in the sense that too many mechanisms are involved and it is not known which mechanism is predominant since they are coupled. So far, no theoretical nor physical model which links together the shock wave before the flame front, turbulence and boundary layer effects has explained the transition phenomenon in a satisfactory manner. Further insight into the problem may be obtained by studying transition under unconfined conditions. The mechanisms that promote transition can be isolated and examined individually.

To investigate the possibility of transition from deflagration to detonation without the benefit of the wall effects, an electric spark ($^{a}0.1$ μ capacitor charged to 4000V and discharged through a 2 mm gap) was used, and the width of the pill box was 3-1/2 inches. The mixture used was 50%-50% acetylene and oxygen. Within the initial pressure range of 5 - 200 mm Hg, no detonation was observed. A typical streak photograph is shown in Figure (31). On discharging the capacitor, a deflagration wave was formed which accelerated to a constant speed of 180 metres per second. Near the inner rim of the cylindrical vessel, the reflection of the pressure waves generated by the flame front interacted with the flame and caused a deceleration of the deflagration wave. This was followed by an instantaneous explosion in the unburnt mixture. Similar results of a violent explosion near the container wall were reported by Cassutt (Reference 9) who detected a sudden pressure rise at the wall of a 6 ft. diameter latex ballon. The fact that transition is not possible has been indicated by the theoretical work of Chu (Reference 11). He extended Taylor's (Reference 12) analysis of an expanding sphere to the case of a spherical flame, and from his numerical data, transition from deflagration to detonation is not possible since an unrealistically high reaction rate is required to produce a shock of sufficient strength to cause auto-ignition behind it.

Results similar to spark ignition were obtained by using a hot wire (0.1 mm diameter, 3-1/2 inches long Ni-C_r resistance wire). The wire was heated to white hot in less than a second by a 36 volts D.C. power supply. Contrary to Friewald's results (Reference 8), no detonation was observed. A streak photograph of the deflagration wave at an initial pressure of 100 mm Hg is shown in Figure (32).

To study the effects of the side walls on transition, the width of the pill box was reduced to 1/2". Spark and hot wire were used to ignite the mixture. Results similar to those for a 3-1/2" wide pill box were observed.

The effect of turbulence on the transition from cylindrical deflagration to detonation was investigated by placing a 1/8" diameter wire in a spiral manner on the inner surface of one of the side walls. The width of the cylindrical vessel was 3-1/2" so that boundary layer effects could be neglected. Hot wire and spark ignition were again used. All experiments were carried out for 50%-50% acetylene and oxygen mixture at an initial pressure range of 5 - 200 mm Hg. A typical streak photograph is shown in Figure (33). Transition to detonation was observed near the inner rim of the pill box. This illustrates the importance of turbulence in the transition phenomenon.

At this stage, it is possible to give a qualitative description of the transition from cylindrical deflagration to detonation with special emphasis to turbulence and wall effects. After the mixture is iginited at the centre of the cylindrical vessel by a spark or hot wire, a flame propagates radially outwards. Initially, laminar burning occurs and since the volume of burnt gas in many times greater than the unburnt mixture, the products of combustion can be treated as a hot gas piston sending out compression waves ahead of the flame. These pressure waves raise the temperature of the unburnt mixture which in turn increases the burning velocity, giving an acceleration to the flame. The compression waves will coalesce to form a shock. The boundary layer between the shock and the flame front will be turbulent

due to the presence of the trip wire placed on the inner surface of one of the side walls of the pill box. The flame then becomes turbulent and there is a further acceleration due to the increase in flame area. The large scale turbulence distorts the flame surface so much that elements of the flame start to break away and pockets of unburnt mixture are left behind the flame front. Intermittent pressure pulses are generated due to the almost instantaneous reaction of these pockets of unburnt mixture. The shock is strengthened continuously by the pressure pulses generated by the turbulent flame front. At the foot of the shock, the temperature will eventually be high enough to cause auto-ignition. A secondary flame will propagate along the boundary layer and behind the shock front. A large volume of unburnt mixture is trapped between the flame front and the secondary flame originated at the foot of the shock. Prior to the onset of detonation, a deflagrative implosion occurs. A strong shock is formed due to the instantaneous reaction. This shock will coalesce with the original shock in front of the flame to form a detonation, while another shock also propagates back towards the burnt gas as a retonation wave.

It should be noted that the above mentioned transition process does not hold under truly unconfined conditions since wall effects and large scale turbulence are absent. The aim of the above mentioned experiments is to determine the most predominant factors in transition to detonation. It is thus possible to predict the possibility of transition from deflagration to detonation under different conditions by knowing whether the basic mechanisms are present or not.

7.6 UNSTABLE PHENOMENA

The possibility of spinning and pulsations in two-dimensional detonation waves was investigated. The first series of experiments were performed under low pressures (5 - 20 mm Hg), and 50%-50% acetylene-oxygen mixtures were used. Cylindrical detonations were initiated by use of exploding wire. The ignition energy was 12.8 joules. No pulsations nor spinning were observed. Similar experiments carried out in a tube showed spinning

and pulsations of the detonation wave within this pressure range.

In the second series of experiments, the initial pressure range was 30 - 50 mm Hg and the mixture composition was the same as the first series. However, the mixture was saturated with water vapour by passing through a water bath before it was bled into the cylindrical vessel. 12.8 joules from the exploding wire were used to ignite the mixture. It was found that spinning and pulsations phenomena were absent when the initial pressure was above 40 mm Hg. Below this pressure, no detonation was formed. The heat of reaction was lowered considerably by the addition of moisture so that it could not sustain a detonation, and only normal burning was observed.

In the third series of experiments, the stability of a cylindrical detonation wave was investigated. 50%-50% acetylene-oxygen mixtures were used and the initial pressure was 100 mm Hg. A kink was introduced in the wave by a 3/8" diameter rod placed across its path at a position 10 inches away from the ignition source. Streak photographs of the cylindrical detonation wave before and after it passed the obstruction did not show any change of speed, and the cylindrical symmetry of the wave was preserved.

7.7 INITIATION ENERGY

The critical energy for the instantaneous initiation of a cylindrical detonation wave was determined for a 50%-50% acetylene-oxygen mixture at an initial temperature and pressure of 300° K and 100 mm Hg respectively. The spark gap was 2 mm wide and the capacitor bank was charged to a potential of 4000V. The energy was varied by changing the value of the capacitors. Streak photographs were taken to determine whether a deflagration or a detonation was formed for each value of initiation energy. For spark ignition, the critical energy was found to be 11.25 joules. This value is higher than the actual critical energy since it is assumed the spark to have a 100% efficiency. There are losses through the electrical leads and the capacitor may not be fully discharged. This experimentally determined value of 11.25 joules can only be taken as a qualitative illustration of the order of magnitude of the energy required to initiate a cylindrical detonation wave.

CHAPTER VIII

CONCLUSIONS

The following conclusions may be drawn from the theoretical analysis and experimental studies of a cylindrical detonation wave:

(a) A sufficiently large amount of energy is required to initiate a cylindrical detonation wave. For 50%-50% acetylene-oxygen mixtures at an initial pressure of 100 mm Hg, the critical spark energy is 11.25 joules when a spark efficiency of 100% is assumed.

(b) For small radius, a cylindrical detonation does not satisfy the Chapman-Jouguet hypothesis. The wave is initially over-driven. It will approach a plane detonation for large radius. The energy law is then satisfied since the ignition energy is negligible compared to the chemical energy released, and the wave propagates with a velocity that corresponds to a plane Chapman-Jouguet detonation.

(c) The velocity is a very insensitive parameter as it is not possible to detect any changes near the centre of the wave. Vertical slit streak photographs and pressure measurements at different radii from the ignition source give more information as to the steadiness of the cylindrical detonation wave.

(d) Pressure measurements of the combustion products taken at radii sufficiently far away from the ignition source agree with the theoretical values based on the similarity solution.

(e) Turbulence and boundary layer effects are the predominant mechanisms in the transition from deflagration to detonation. Without these effects, transition is not possible since an unrealistically high reaction rate is required to produce a shock of sufficient strength to cause auto-ignition behind it.

(f) Spinning and pulsating phenomena in two-dimensional detonation waves are absent for moist 50%-50% acetylene-oxygen mixtures between the initial pressure range of 5 - 20 mm Hg. Similar experiments performed in

a tube show that the wave spins and pulsates.

(1) The perfect symmetrical wave shape is not distorted by the introduction of a small obstacle placed across the detonation path.

CHAPTER IX

RECOMMENDATIONS

A truly Chapman-Jouguet detonation wave is not realizable experimentally in a tube because of the presence of wall effects which causes the flow in and behind the reaction zone to be turbulent. A cylindrical detonation wave has the distinct advantage that these effects are kept to such a minimum that they have hardly any effect on the wave. Instantaneous spark Schlierens and interferograms of the reaction zone will reveal more information as to the structure of detonation waves than could be obtained from plane detonations confined in tubes. A closer agreement with the present theoretical models can therefore be obtained. Future experiments should also include time resolved spectroscopic studies of the reaction zone in order that the concentration profiles can be determined and hence a better understanding of detonation waves in general can be achieved.

To further understand the formation of unconfined detonation waves, the initiation mechanisms should be investigated in more detail. A theoretical model should be formulated by considering the detonation to be a blast wave initially and decays to a steady self-sustained detonation wave when the chemical energy released becomes dominant as compared to the initiation energy. A relationship between the initiation energy and chemical energy could be found so that it is possible to predict at what distance from the ignition source would the overdriven detonation decay to a Chapman-Jouguet detonation. Further experimental investigations should also be carried out to verify the theoretical model by measuring the distance from the ignition source where a steady Chapman-Jouguet cylindrical detonation wave is formed for different fuel-oxygen reactive mixtures and for different initiation energies.

APPENDIX I

DERIVATION OF THE GASDYNAMIC EQUATIONS OF FLUID MOTION

In the generalized derivation of the equations of fluid motion, vector and tensor notations are used.

The Mass Conservation Law

Consider an arbitrary fixed volume V in space surrounded by a surface S (Figure 6). Then the conservation of mass requires that the net flow across S must be equal to the change in mass in V.

Let the velocity at any point on S be $\vec{q}$; further, let $\vec{n}$ be the unit vector normal to the surface. The mass flux across S is

$$\iint_S \rho(\vec{n}\cdot\vec{q})\,dS$$

and the rate of change of mass inside S is

$$\iiint_V \frac{\partial \rho}{\partial t}\,dV$$

Thus mass is conserved if

$$-\iint_S \rho(\vec{n}\cdot\vec{q})\,dS = \iiint_V \frac{\partial \rho}{\partial t}\,dV \qquad \ldots\ldots (70)$$

Using Gauss Theorem which relates a surface integral to a volume integral, the continuity equation becomes:

$$\iiint_V \left(\frac{\partial \rho}{\partial t} + \nabla\cdot\rho\vec{q}\right) dV = 0$$

or

$$\frac{\partial \rho}{\partial t} + \nabla\cdot\rho\vec{q} = 0 \qquad \ldots\ldots (71)$$

The Momentum Conservation Equation

This law is an analytic formulation for a fluid of Newton's second law. Considering again the control volume V enclosed by the surface S, the rate of change of momentum $(d\vec{M}/dt)$ is equal to the momentum flux across the boundary ($\iint_S \rho\vec{q}(\vec{n}\cdot\vec{q})\,dS$) and the time rate of change of momentum inside V ($\iiint_V \frac{\partial\rho\vec{q}}{\partial t}\,dV$)

Thus

$$\frac{d\vec{M}}{dt} = \iint_S \rho\vec{q}(\vec{n}\cdot\vec{q})\,dS + \iiint_V \frac{\partial\rho\vec{q}}{\partial t}\,dV \qquad \ldots\ldots(72)$$

which by Gauss theorem can be written:

$$\frac{d\vec{M}}{dt} = \iiint_V \left(\rho\vec{q}(\nabla\cdot\vec{q}) + (\vec{q}\cdot\nabla)\rho\vec{q} + \frac{\partial\rho\vec{q}}{\partial t}\right)dV \qquad \ldots\ldots(73)$$

Using the mass conservation equation, this equation can be written as:

$$\frac{d\vec{M}}{dt} = \iiint_V \left(\frac{d\rho\vec{q}}{dt} - \vec{q}\,\frac{d\rho}{dt}\right)dV$$

$$= \iiint_V \rho\,\frac{d\vec{q}}{dt}\,dV \qquad \ldots\ldots(74)$$

where $$\frac{d}{dt} \equiv \frac{\partial}{\partial t} + (\vec{q}\cdot\nabla) \qquad \ldots\ldots(75)$$

The external forces acting on the fluid are the gravitational forces and the mechanical surface forces. For a Newtonian fluid, the gravitational force is $\iiint_V \rho \vec{F}\, dV$. The mechanical surface forces include the pressure and the viscous forces and can be written as $\iint_S \tau_{ij}\, ds_i$, where τ_{ij} is a tensor quantity.

From Gauss theorem,

$$\iint_S \tau_{ij}\, ds_i = \iiint_V \frac{\partial}{\partial x_j} \tau_{ij}\, dV \qquad \ldots\ldots (76)$$

But τ_{ij} consists of the pressure and viscous terms and can be expressed as:

$$\tau_{ij} = -p\,\delta_{ij} + \tau_{ij}^{vis.} \qquad \ldots\ldots (77)$$

where δ_{ij} is the Kronecker delta

and $\delta_{ij} = 1$ when $i = j$

$= 0$ when $i \neq j$

For an inviscid fluid, $\tau_{ij}^{vis.} = 0$ so that

$$\frac{\partial \tau_{ij}}{\partial x_j} = -\nabla p$$

The general law of momentum conservation for an inviscid , compressible fluid is then

$$\rho \frac{d\vec{q}}{dt} = \rho \vec{F} - \nabla p \qquad \ldots\ldots (78)$$

The Energy Conservation Law

The rate at which forces do work on a volume of fluid is equal to the rate of increase of the kinetic energy and internal energy plus the rate of conduction of heat across the fluid boundary. Again using the arbitrary volume V and surface S, the work done on the fluid is through transportation of the body forces and transportation of the internal stress forces.

Rate at which work is done on the fluid volume minus the rate of increase of kinetic energy

$$= \iiint_V \left\{ -p(\nabla \cdot \vec{q}) + \Phi \right\} dV$$

where Φ is known as the dissipation function.

The rate of increase of internal energy is given by the relation

$$\frac{d}{dt} \iiint_V \rho E \, dV$$

where E is the specific internal energy.

The heat conduction across the boundary is given by the expression

$$- \iint_S k \frac{\partial T}{\partial n} \, dS$$

Thus the energy equation may be written as:

$$\frac{d}{dt} \iiint_V \rho E \, dV = \iiint_V \left\{ -p(\nabla \cdot \vec{q}) + \Phi \right\} dV + \iint_S k \frac{\partial T}{\partial n} \, dS \qquad \ldots\ldots (79)$$

Using the continuity equation and the Gauss theorem, one obtains,

$$\rho \frac{dE}{dt} = -p(\nabla \cdot \vec{q}) + \Phi + (\nabla \cdot k \nabla) T \qquad \ldots\ldots (80)$$

APPENDIX II

DERIVATION OF THE GASDYNAMIC EQUATIONS FOR CYLINDRICAL DETONATION WAVES

GOVERNING EQUATIONS

The fundamental equations governing the flow behind a cylindrical detonation wave can be obtained from Equations (34) and (35) by setting $j = 1$. They are:

Mass Conservation

$$\frac{\partial \rho}{\partial t} + u\frac{\partial \rho}{\partial r} + \rho\left(\frac{\partial u}{\partial r} + \frac{u}{r}\right) = 0$$

Momentum Conservation

$$\frac{\partial u}{\partial t} + u\frac{\partial u}{\partial r} + \frac{1}{\rho}\frac{\partial p}{\partial r} = 0$$

In Section 4.4, a similarity parameter $\frac{r}{t}$ is derived. Let $x = r/t$, then partial differentiation with respect to r and t can be written as:

$$\frac{\partial}{\partial r} = \frac{1}{t}\frac{d}{dx} \qquad \ldots\ldots (81)$$

$$\frac{\partial}{\partial t} = -\frac{x}{t}\frac{d}{dx} \qquad \ldots\ldots (82)$$

Using Equations (81) and(82), the conservation laws can be expressed as:

$$\left(\frac{u-x}{\rho}\right)\frac{d\rho}{dx} + \frac{du}{dx} + \frac{u}{x} = 0 \qquad \ldots\ldots (83)$$

$$(u-x)\frac{du}{dx} + \frac{1}{\rho}\frac{dp}{dx} = 0 \qquad \ldots\ldots (84)$$

Since a perfect gas is considered, the speed of sound $c^2 = dp/d\rho$, and $d\rho/dx$ can be eliminated from Equations (83) and (84) to give

$$\frac{du}{dx}\left\{1 - \left(\frac{x-u}{c}\right)^2\right\} = -\frac{u}{x} \qquad \text{.....(85)}$$

Define:

$$\xi = \frac{u}{x} \quad , \quad \eta = \frac{c^2}{x^2} \quad , \quad Z = \ln x \qquad \text{.....(86)}$$

and substitute into Equation (85) gives the expression

$$\frac{du}{dx}\left\{1 - \frac{1}{\eta}(1-\xi)^2\right\} = -\xi \qquad \text{..... (87)}$$

Differentiating ξ, η and Z with respect to x, one obtains the following equations:

$$\frac{du}{dx} = \xi + x\frac{d\xi}{dx} \qquad \text{..... (88)}$$

$$\frac{dc^2}{dx} = 2x\eta + x^2\frac{d\eta}{dx} \qquad \text{.....(89)}$$

$$\frac{dZ}{dx} = \frac{1}{x} \qquad \text{..... (90)}$$

These 3 Equations when substituted in Equation (87) and (83) give:

$$\frac{dZ}{d\xi} = -\frac{1}{\xi}\left\{\frac{\eta - (1-\xi)^2}{2\eta - (1-\xi)^2}\right\} \qquad \text{.....(91)}$$

and

$$\frac{x}{fc^2}(1-\xi)\left(2x\eta + x^2\frac{d\eta}{dx}\right) = 2\xi + x\frac{d\xi}{dx} \qquad \text{.....(92)}$$

where $$f = \frac{\gamma dc^2}{c^2 d\varphi}$$

For a perfect gas, p/ρ^γ = constant, and after simplification $f = \gamma - 1$.

The term $x\frac{d\xi}{dx}$ in Equation (92) is simply $\frac{d\xi}{dZ}$.

The substitution of Equation (91) into Equation (92) gives the following expression:

$$\frac{d\eta}{d\xi} = \frac{\eta}{\xi}\left\{\frac{2\eta - 2(1-\xi)^2 + f\xi(1-\xi)}{2\eta - (1-\xi)^2}\right\} \qquad \text{.....(93)}$$

In order to simplify Equations (90) and (93), define $\psi = u/c$ so that $\eta = \xi^2/\psi^2$. Substituting the new value of η into Equation (91) gives:

$$\frac{d\xi}{dZ} = \xi\left\{\frac{2\xi^2 - (1-\xi)^2\psi^2}{(1-\xi)^2\psi^2 - \xi^2}\right\} \qquad \text{.....(94)}$$

The derivative of η is:

$$\frac{d\eta}{d\xi} = \frac{2\xi}{\psi^2} - \frac{2\xi^2}{\psi^3}\frac{d\psi}{d\xi}$$

and combining with Equations (93) and 94) yields:

$$\frac{d\psi}{dZ} = \frac{\xi\psi}{2}\left\{\frac{2\xi - (1-\xi)f\psi^2}{(1-\xi)^2\psi^2 - \xi^2}\right\} \qquad \text{.....(95)}$$

APPENDIX III

THE RUNGE-KUTTA METHOD

The Runge-Kutta Method (Reference 29) is a step by step approximation. It has the advantage that no initial values are needed beyond the prescribed values. Equations (94) and (95) can be written in the following form;

$$\frac{d\xi}{dZ} = f(\xi, \psi) \qquad \text{.....(96)}$$

$$\frac{d\psi}{dZ} = g(\xi, \psi) \qquad \text{.....(97)}$$

The coefficients used in this method are defined as:

$$\begin{aligned}
c_{11} &= \Delta Z\, f(\xi_0, \psi_0) \\
c_{21} &= \Delta Z\, f(\xi_0 + c_{11}/2, \psi_0 + c_{12}/2) \\
c_{31} &= \Delta Z\, f(\xi_0 + c_{21}/2, \psi_0 + c_{22}/2) \\
c_{41} &= \Delta Z\, f(\xi_0 + c_{31}, \psi_0 + c_{32}) \\
c_{12} &= \Delta Z\, g(\xi_0, \psi_0) \\
c_{22} &= \Delta Z\, g(\xi_0 + c_{11}/2, \psi_0 + c_{12}/2) \\
c_{32} &= \Delta Z\, g(\xi_0 + c_{21}/2, \psi_0 + c_{22}/2) \\
c_{42} &= \Delta Z\, g(\xi_0 + c_{31}, \psi_0 + c_{32})
\end{aligned} \qquad \text{.....(98)}$$

where ξ_0, ψ_0 and Z_0 are the starting values, and ΔZ is the interval.

For each increment of Z, ξ and ψ are given as follows:

$$\xi = \xi_0 + \frac{1}{6}\left(C_{11} + 2C_{21} + 2C_{31} + C_{41}\right) \qquad \ldots\ldots (99)$$

$$\psi = \psi_0 + \frac{1}{6}\left(C_{12} + 2C_{22} + 2C_{32} + C_{42}\right)$$

The corresponding value of r/R is obtained by taking the anti-

logarithm of $Z + \Delta Z$.

APPENDIX IV

REFERENCES

1. M. Jouguet	Comptes Rendus Vol. 142, 1906
2. Laffitte, P.	Ann. de Phys., 10e ser 4, 587(1925)
3. Taylor, G.I.	The Dynamics of the Combustion Products behind Plane and Spherical Detonation Fronts in Explosives Proc. Roy. Soc. A200, 1950
4. Zeldovich, Ia.B, and Kompaneets, A.S.	Theory of Detonation Academic Press
5. Manson, N. and Ferrie, F.	Contribution to the Study of Spherical Detonation Waves Fourth Symposium on Combustion 1953
6. Litchfield, E.L.	Freely Expanding Gaseous Detonation Waves Initiated by Electric Discharges Phys. of Fluids Vol.5 No. 1, 1963
7. Litchfield, E.L., Hay, M.H., and Forshey, D.R.	Direct Electrical Initiation of Freely Expanding Gaseous Detonation Waves Ninth International Symposium on Combustion
8. Freiwald, H. and Koch, H.W.	Spherical Detonations of Acetylene-Oxygen-Nitrogen Mixtures as a Function of Nature and Strength of Initiation Ninth International Symposium on Combustion
9. Cassutt, L.H.	Experimental Investigation of Detonation in Unconfined Gaseous Hydrogen-Oxygen-Nitrogen Mixtures ARS Journal Vol. 31 No. 8, 1961
10. Macek, A.	Effect of Additives on Formation of Spherical Detonation Waves in Hydrogen-Oxygen Mixtures AIAA Journal Vol 1 No.8, 1963
11. Chu, B.T.	Pressure Waves Generated by Addition of Heat in a Gaseous Medium NACA TN 3411, 1955
12. Taylor, G.I.	The Air Wave Surrounding an Expanding Sphere Proc. Roy. Soc. A186, 1946

13. von Neumann, J. — Theory of Detonation
John von Neumann Collected Works Vol. VI
Pergamon Press 1963

14. Eisen, C.L., Gross, R.A., and Rivlin, T.J. — Theoretical Calculations in Gaseous Detonation
Combustion and Flame

15. Fay, J.A. — Two-Dimensional Gaseous Detonation: Velocity Deficit
Phys. of Fluids Vol. 2 No. 3, 1959

16. White, D.R. — Turbulent Structure of Gaseous Detonation
Phys. of Fluids Vol. 4 No. 4, 1961

17. Edwards, D.H., Williams, G.T., and Breeze, J.C. — Pressure and Velocity Measurements on Detonation Waves in Hydrogen-Oxygen Mixtures
J. Fluid. Mech. Vol. 6, 1959

18. Edwards, D.H., Jones, T.G., and Price, B. — Observations on Oblique Shock Waves in Gaseous Detonations
J. Fluid. Mech. Vol. 17, Part 1.

19. Emmons, H.W. — Fundamentals od Gas Dynamics
Princeton University Press, 1958

20. Taylor, G.I. — The Formation of a Blast Wave by a very Intense Explosion
Proc. Roy. Soc. A201, 1950

21. Lin, S.C. — Cylindrical Shock Waves Produced by Instantaneous Energy Release
J. Appl. Phys. Vol. 25No. 1, 1954

22. Bollinger, L.E., Fong, M.C., and Edse, R. — Experimental Measurements and Theoretical Analysis of Detonation Induction Distances
ARS Journal Vol. 31 No. 5, 1961

23. Zeleznik, F.J., and Gordon, S. — Calculation of Detonation Properties and Effect of Independent Parameters on Gaseous Detonations
ARS Journal Vol. 32, No. 4, 1962

24. Brinkley, S.R., and Lewis, B. — On the Transition from Deflagration to Detonation
Seventh Symposium on Combustion 1959

25. Laderman, A.J., and Oppenheim, A.K. — Influence of Wave Reflections on the Development of Detonation
Phys. Fluids Vol. 4 No. 6, 1961

26. Jones, H. — Accelerated Flames and Detonation in Gases. Proc. Roy. Soc. A248, 1958

27. Adams, G.K., and Pack, D.C. — Some Observations on the Problem of Transition between Deflagration and Detonation. Seventh Symposium on Combustion 1959

28. Laderman, A.J., and Oppenheim, A.K. — Initial Flame Acceleration in an Explosive Gas. Proc. Roy. Soc. A268

29. Hildebrand, F.B. — Advanced Calculus for Engineers

APPENDIX V

TABULATION OF RESULTS

Table 1. Numerical Solution of the Fluid Properties behind a Cylindrical Detonation Wave

r/R	u/D	c/D	p/p_1	ρ/ρ_1	T/T_1
1.000	.4650	.5350	1.0000	1.0000	1.0000
.999	.4495	.5332	.9527	.9581	.9944
.998	.4433	.5328	.9400	.9467	.9929
.997	.4385	.5325	.9300	.9378	.9916
.996	.4344	.5322	.9215	.9302	.9906
.995	.4308	.5320	.9140	.9235	.9897
.990	.4163	.5309	.8844	.8970	.9859
.950	.3509	.5262	.7569	.7815	.9684
.900	.2964	.5221	.6612	.6935	.9535
.850	.2503	.5187	.5889	.6259	.9409
.800	.2081	.5155	.5295	.5697	.9294
.750	.1682	.5125	.4790	.5213	.9188
.700	.1301	.5097	.4356	.4793	.9088
.650	.0937	.5071	.3982	.4427	.8994
.600	.0592	.5047	.3662	.4111	.8908
.550	.0272	.5025	.3396	.3845	.8831
.500	0	.5008	.3200	.3648	.8771

Table II Experimental Velocities for Plane and Cylindrical Detonations in Acetylene-Oxygen Mixtures. Initial Pressure=100 mm Hg. Initial Temperature=300°K

$\%C_2H_2$ by volume	D_{plane} metres/sec	$D_{cyl.}$ metres/sec	$D_{pl.}-D_{cyl.}$ metres/sec.
20	2120	2100	20
25	2240	2160	80
28.5	2340	2320	20
35	2500	2500	0
40	2610	2590	20
45	2740	2670	70
50	2800	2820	-20
55	2600	2650	-50
60	2460	2350	110

Table 111 Pressure Measurements at 8 cm and 12 cm from Ignition Source

Time in μseconds	p/p_1 (trans. 8 cm from centre)	Experimental Error	p/p_1 (trans. 12 cm from centre)	Experimental Error
2	.800	± .020	.800	± .020
4	.650	± .020	.700	± .030
6	.590	± .030	.645	± .025
8	.545	± .025	.600	± .025
12	.515	± .020	.555	± .035
16	.500	± .040	.515	± .030
20	.465	± .025	.495	± .015
24	.445	± .030	.475	± .025
28	.430	± .040	.470	± .030
32	.415	± .040	.450	± .030
36	.390	± .030	.430	± .020
40	.380	± .040	.400	± .030
44	.370	± .030	.395	± .025
48	.370	± .020	.370	± .020
52	.350	± .020	.370	± .020
56	.325	± .025	.360	± .020
60	.315	± .025	.355	± .020
64	.310	± .030	.350	± .020
68	.300	± .040	.340	± .025
72	.300	± .030	.330	± .020
76	.275	± .025	.310	± .020
80	.270	± .025	.305	± .025
84	.265	± .030	.300	± .020
88	.265	± .030	—	—
90	—	—	.290	± .020
92	.265	± .030	—	—

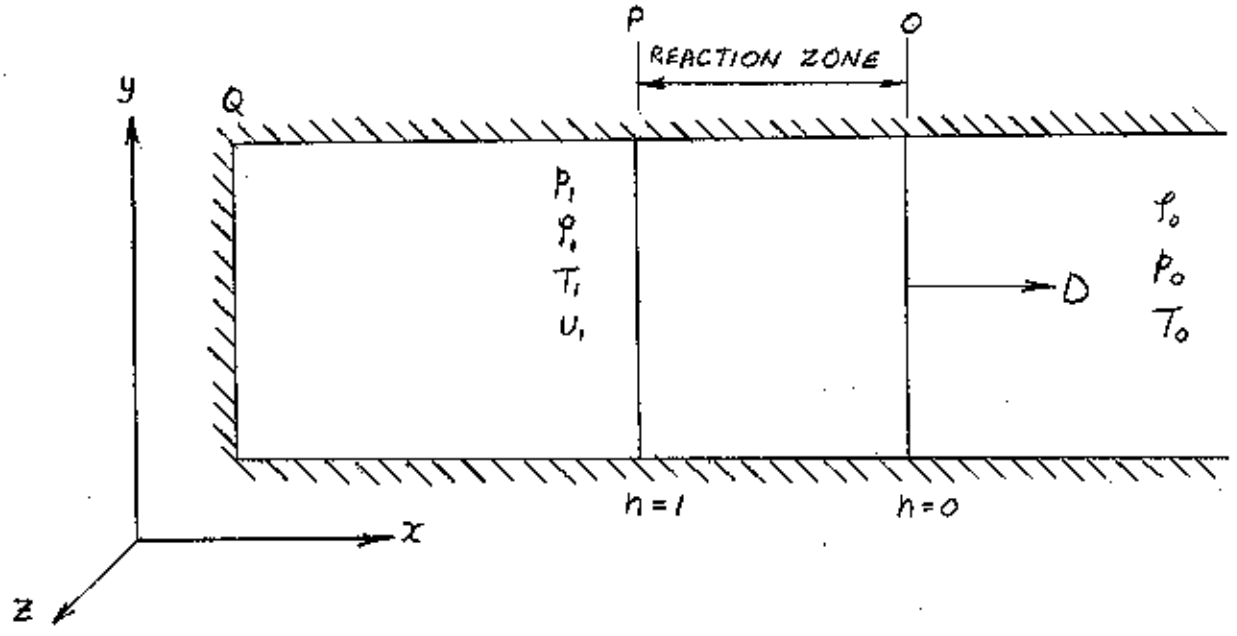

FIGURE 1a NON-STATIONARY DETONATION WAVE

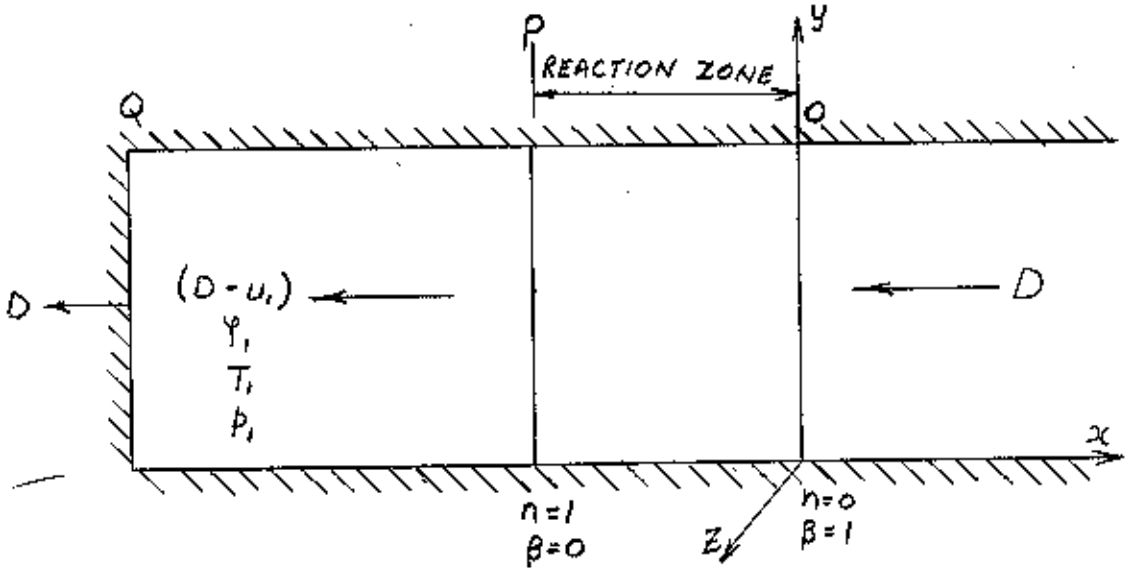

FIGURE 1b STATIONARY DETONATION WAVE

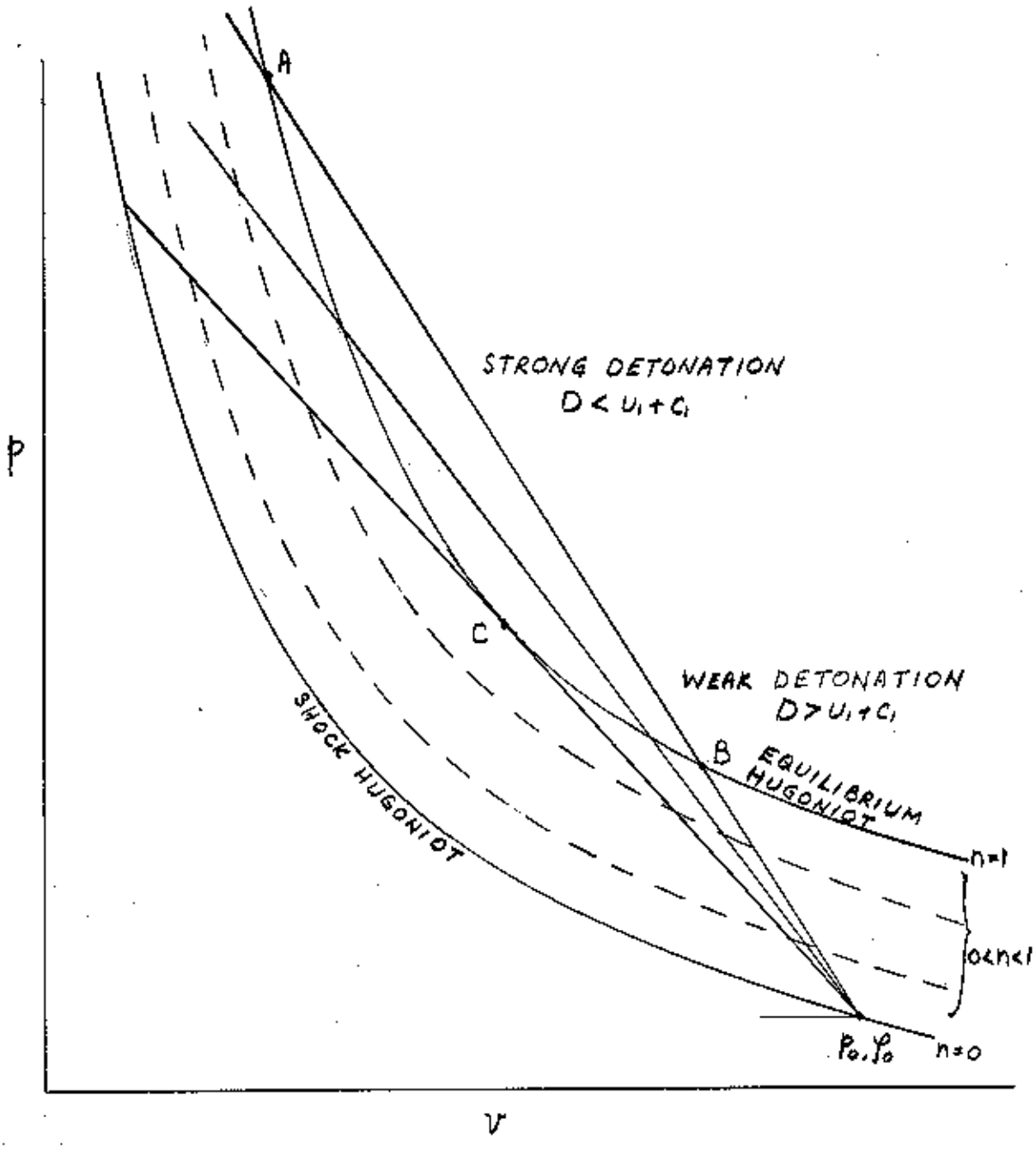

FIGURE 2 RANKINE-HUGONIOT CURVE

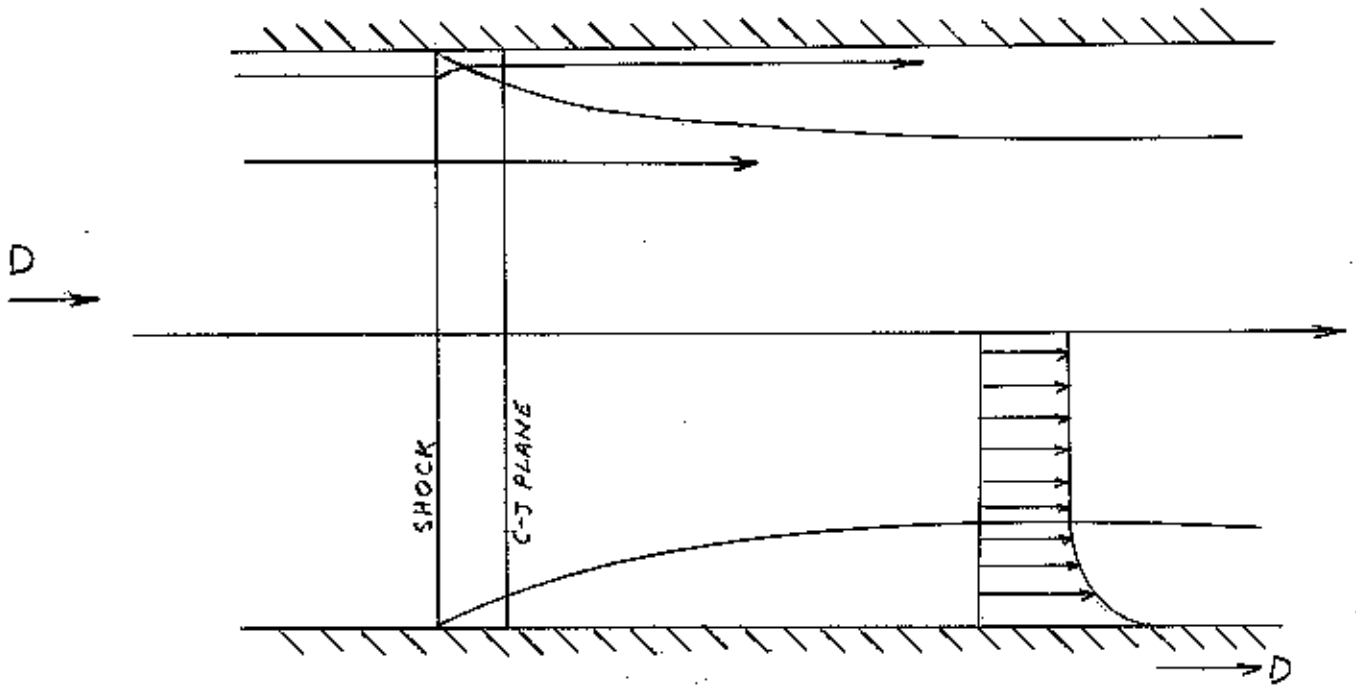

FIGURE 3 STEADY FLOW IN A DETONATION WAVE NEAR THE TUBE WALL

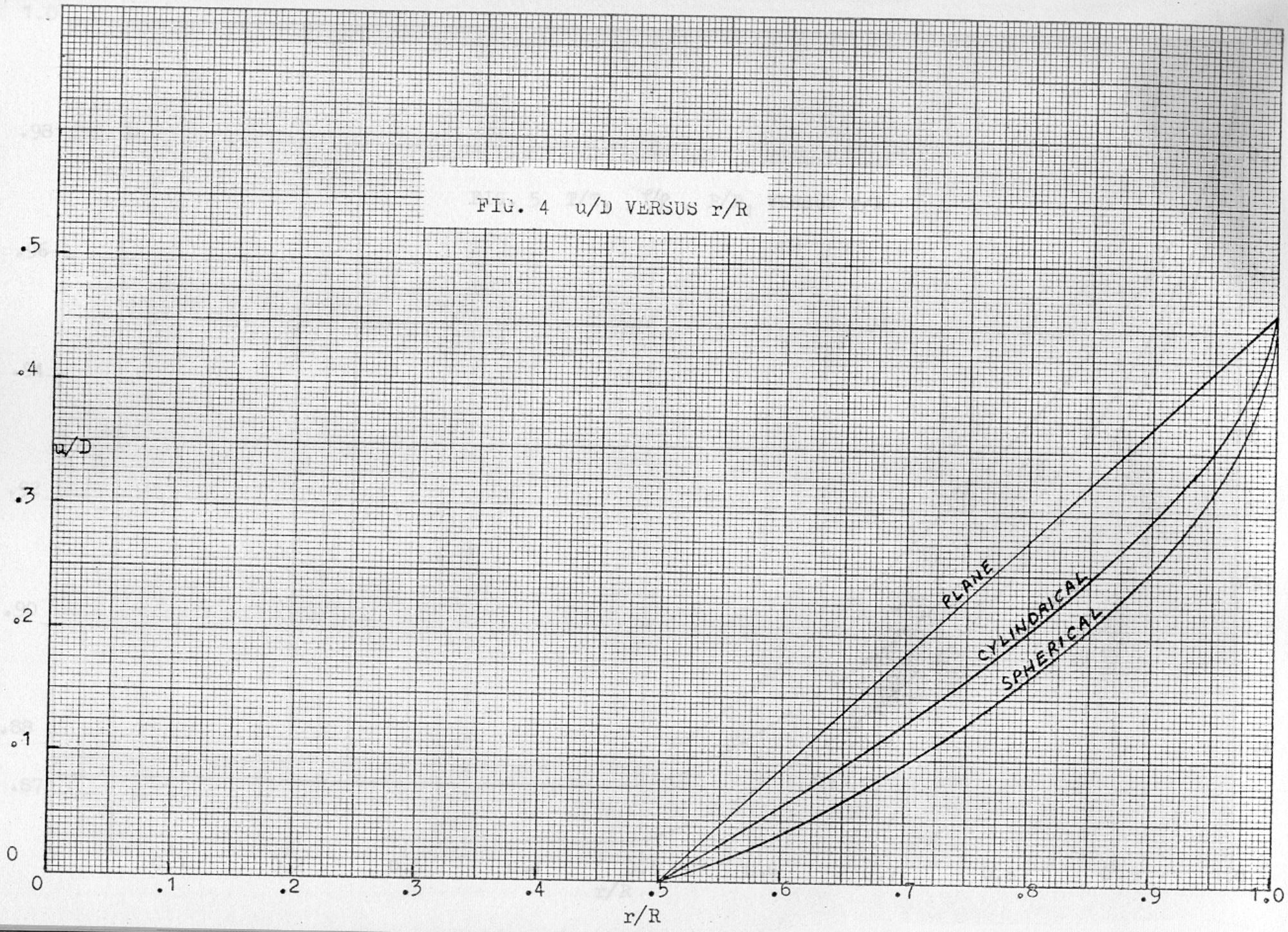
FIG. 4 u/D VERSUS r/R
.5
.4
u/D
.3
.2
.1
0
0
.1
.2
.3
.4
.5
.6
.7
.8
.9
1.0
r/R
PLANE
CYLINDRICAL
SPHERICAL

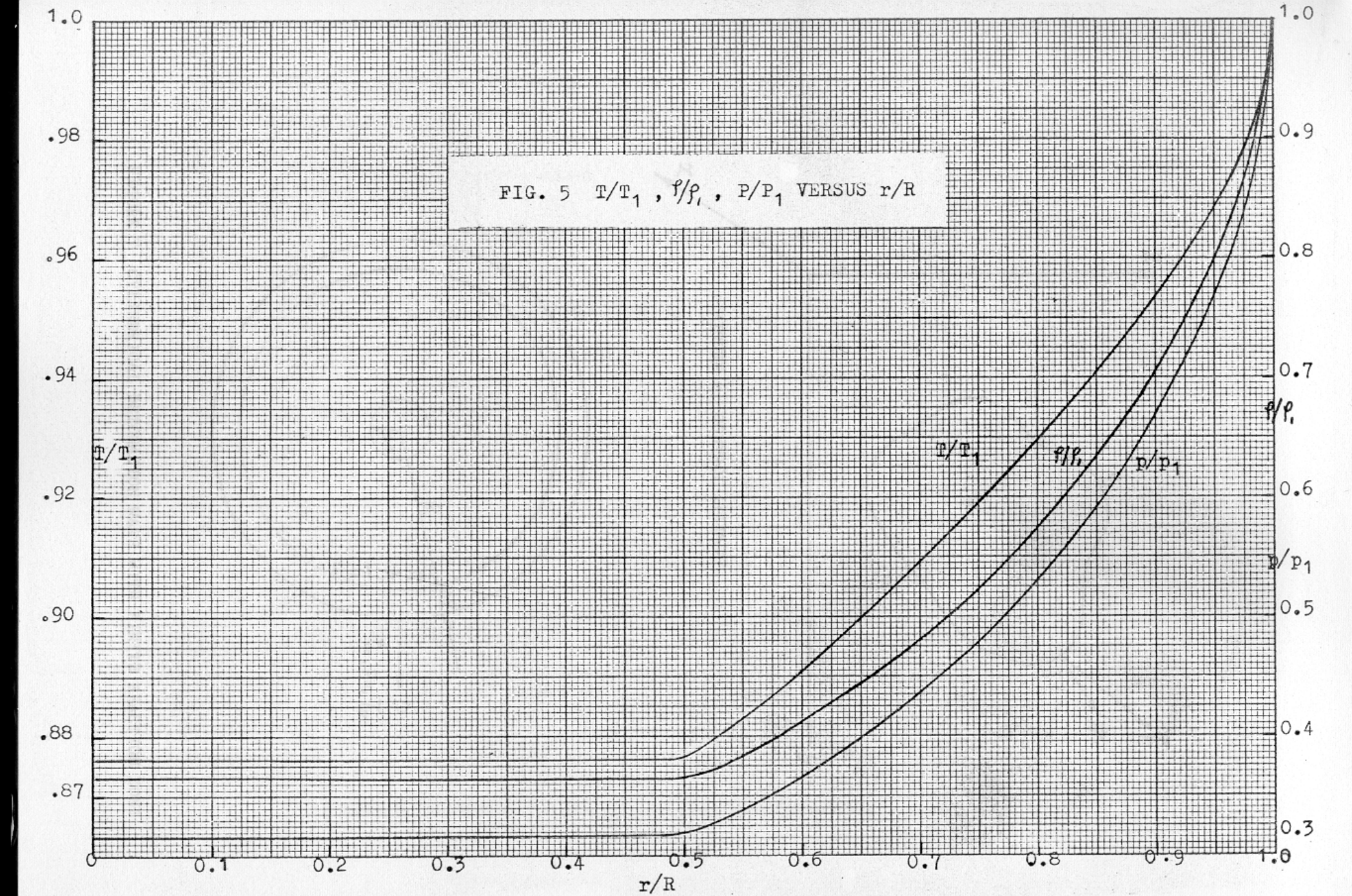
FIG. 5 T/T_1 , ρ/ρ_1 , P/P_1 VERSUS r/R
1.0
.98
.96
.94
.92
.90
.88
.87
T/T_1
1.0
0.9
0.8
0.7
ρ/ρ_1
0.6
P/P_1
0.5
0.4
0.3
0
0.1
0.2
0.3
0.4
0.5
0.6
0.7
0.8
0.9
1.0
r/R
T/T_1
ρ/ρ_1
P/P_1

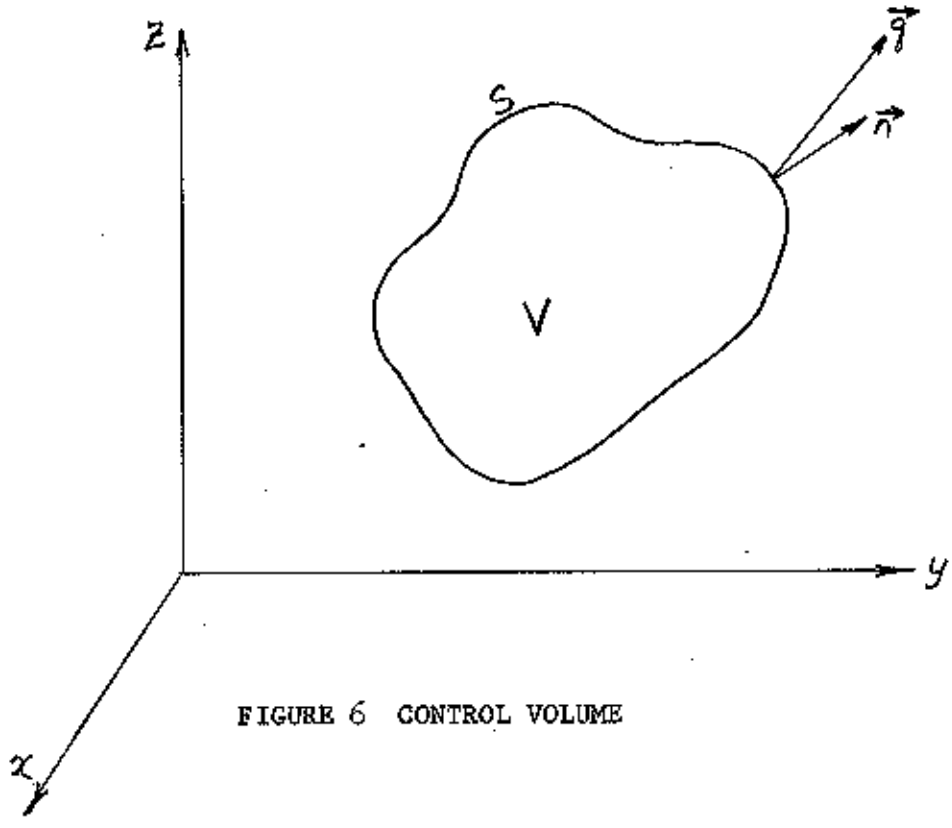

FIGURE 6 CONTROL VOLUME

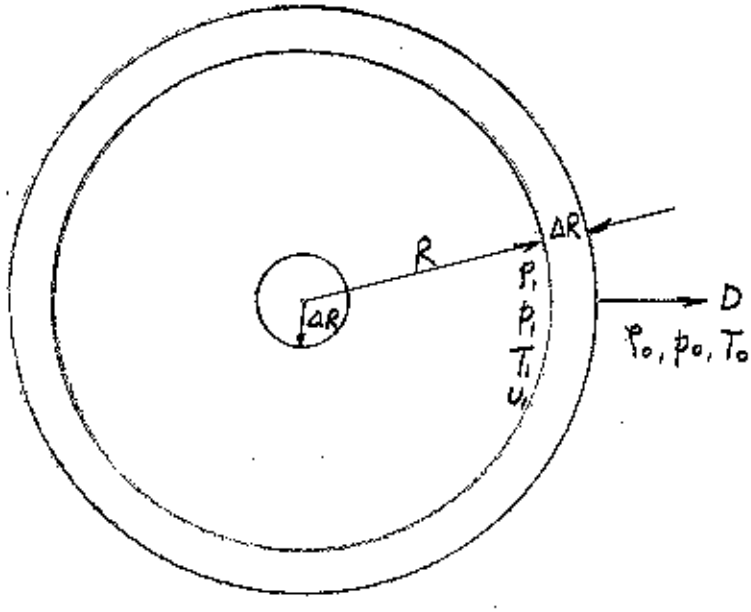

FIGURE 7 CYLINDRICAL DETONATION WAVE WITH FINITE REACTION ZONE

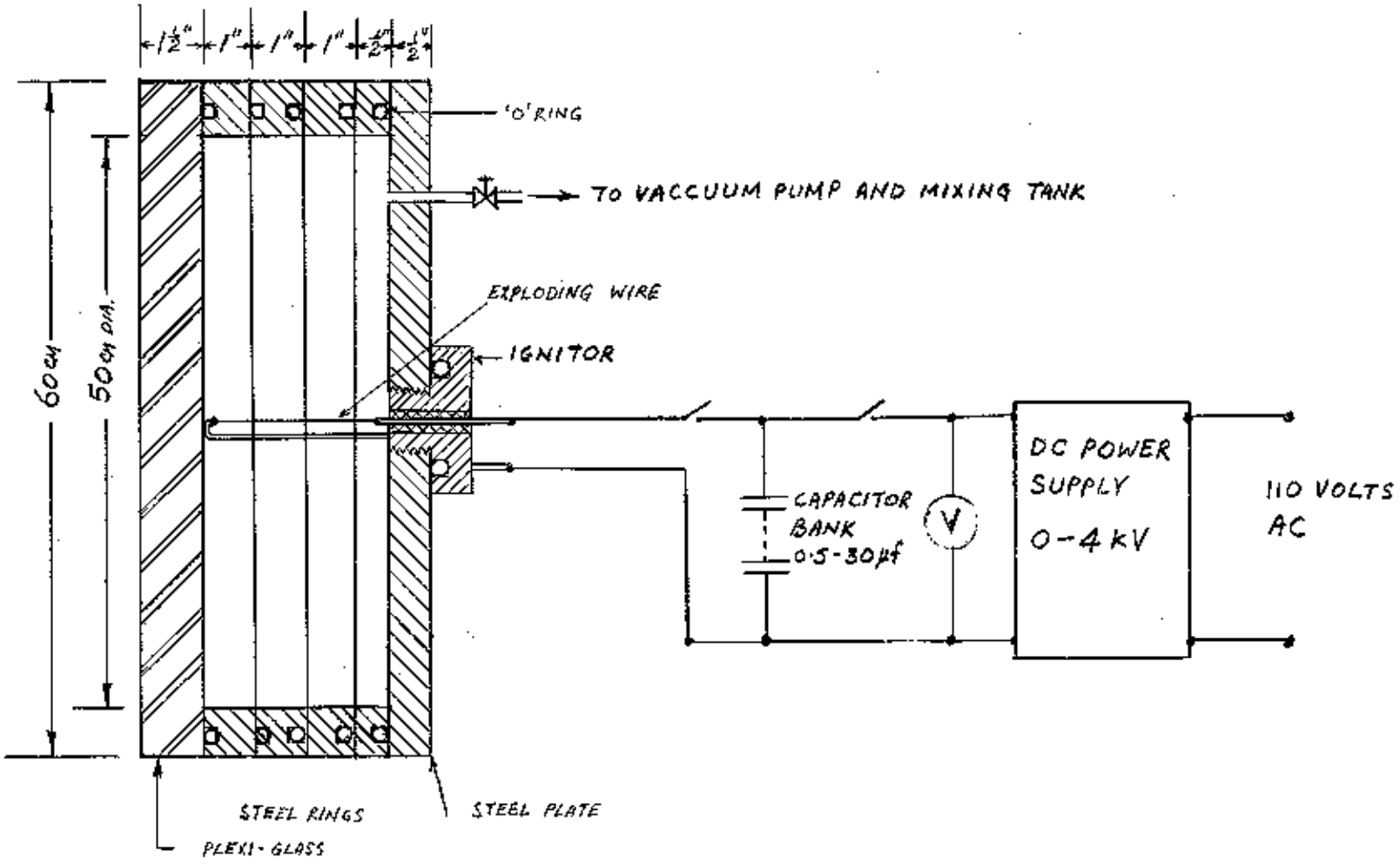

FIGURE 8 SCHEMATIC DIAGRAM OF THE EXPERIMENTAL SET-UP

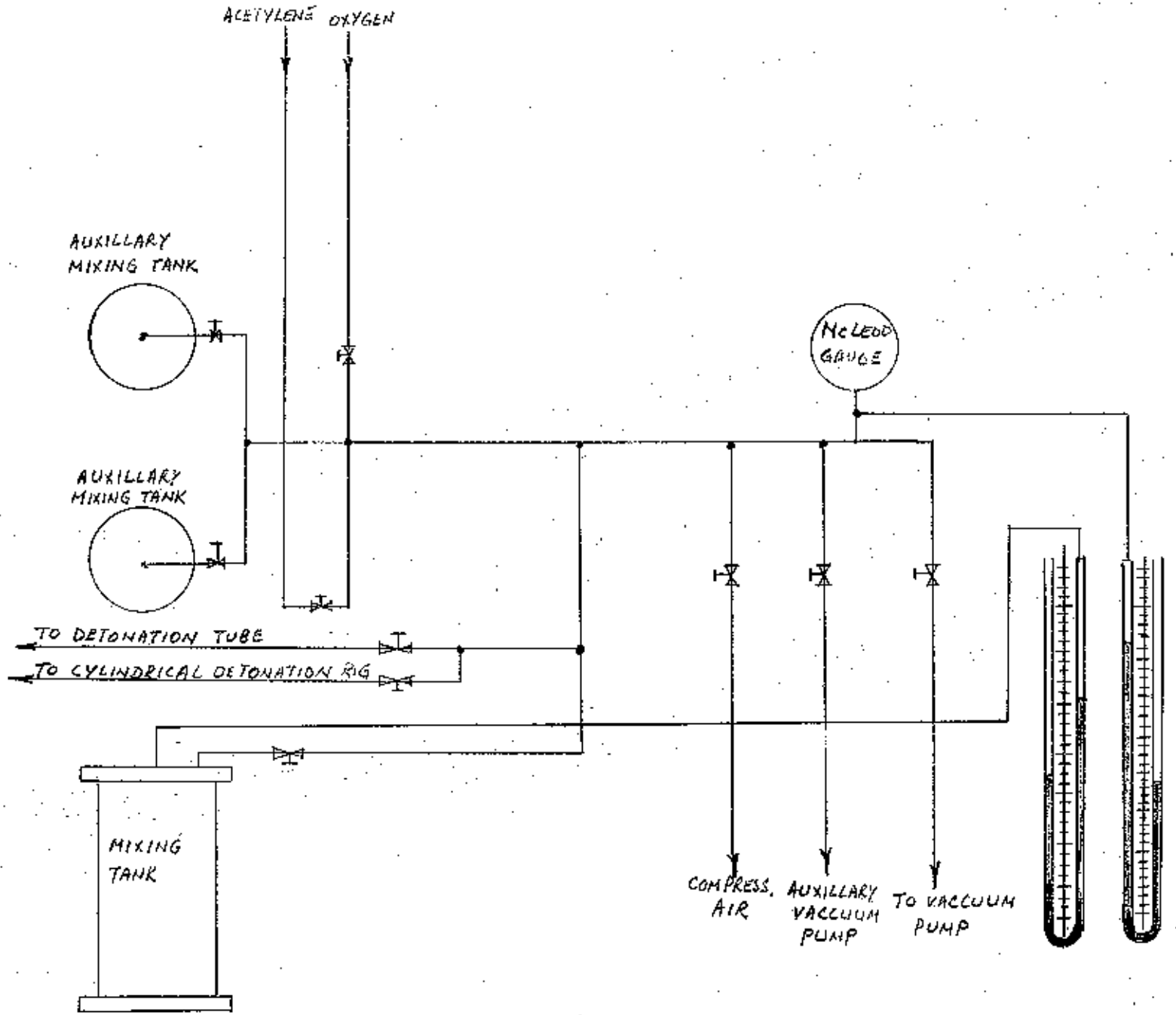

FIGURE 9 DETONATION CONTROL PANEL SCHEMATIC

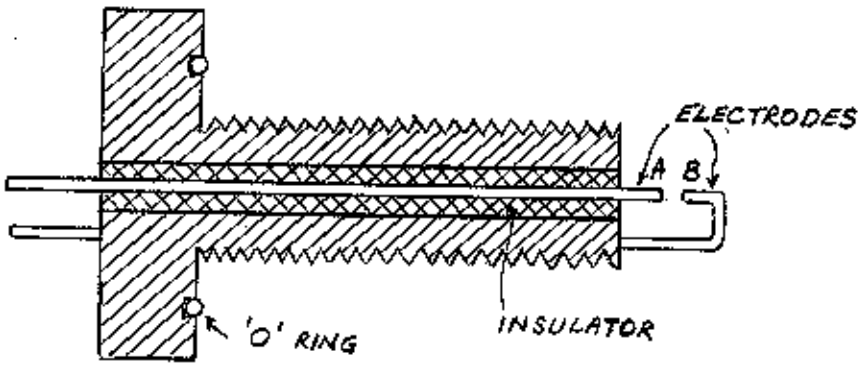

FIGURE 10 SKETCH OF IGNITOR

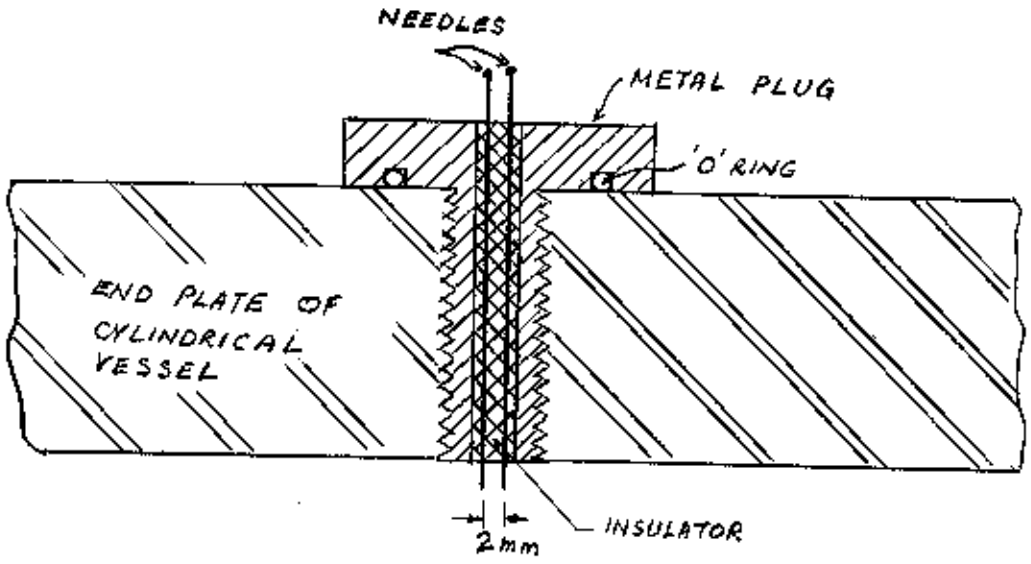

FIGURE 11 IONIZATION PROBE

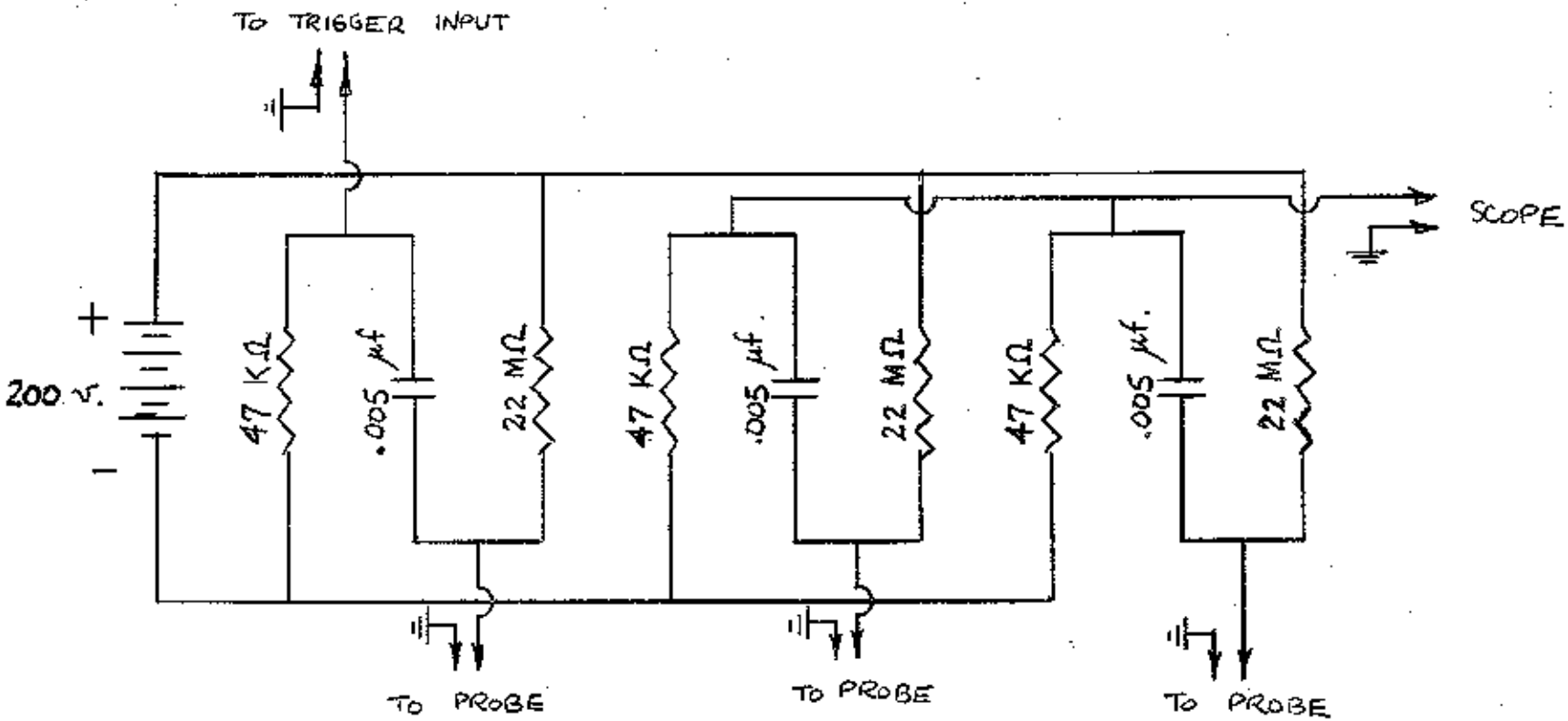

FIGURE 12. IONIZATION PROBE CIRCUIT

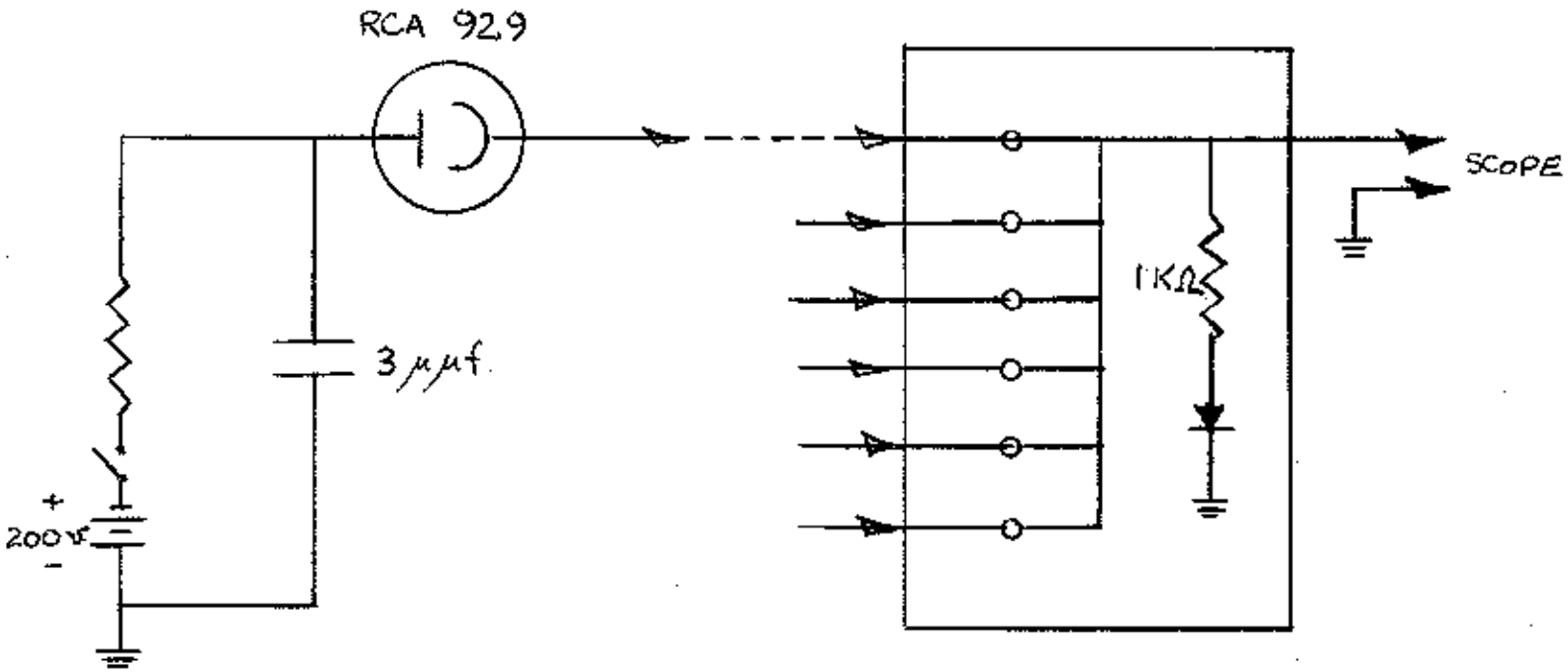

FIGURE 13 PHOTO-TUBE CIRCUIT

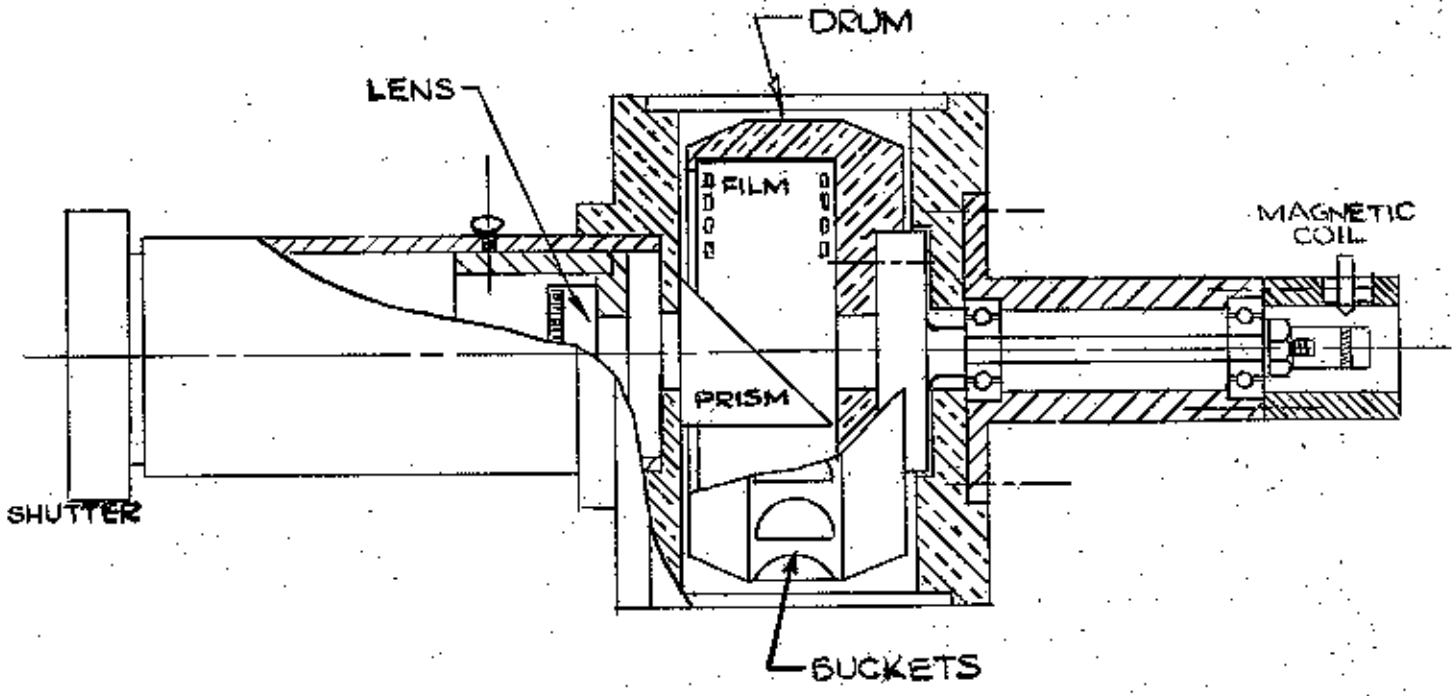

FIGURE 14 ROTATING DRUM STREAK CAMERA

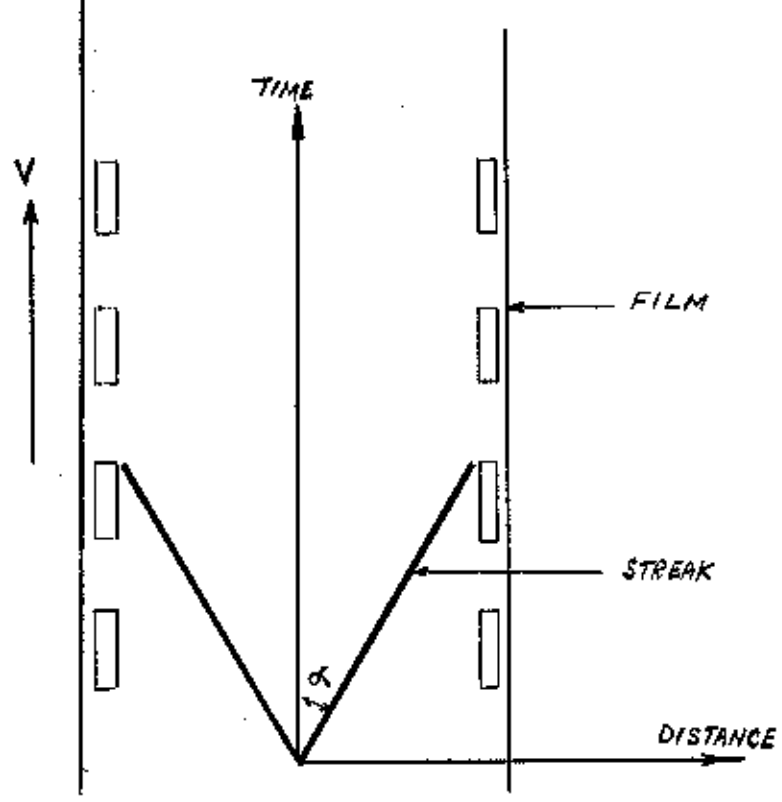

FIGURE 15 STREAK PHOTOGRAPH SCHEMATIC

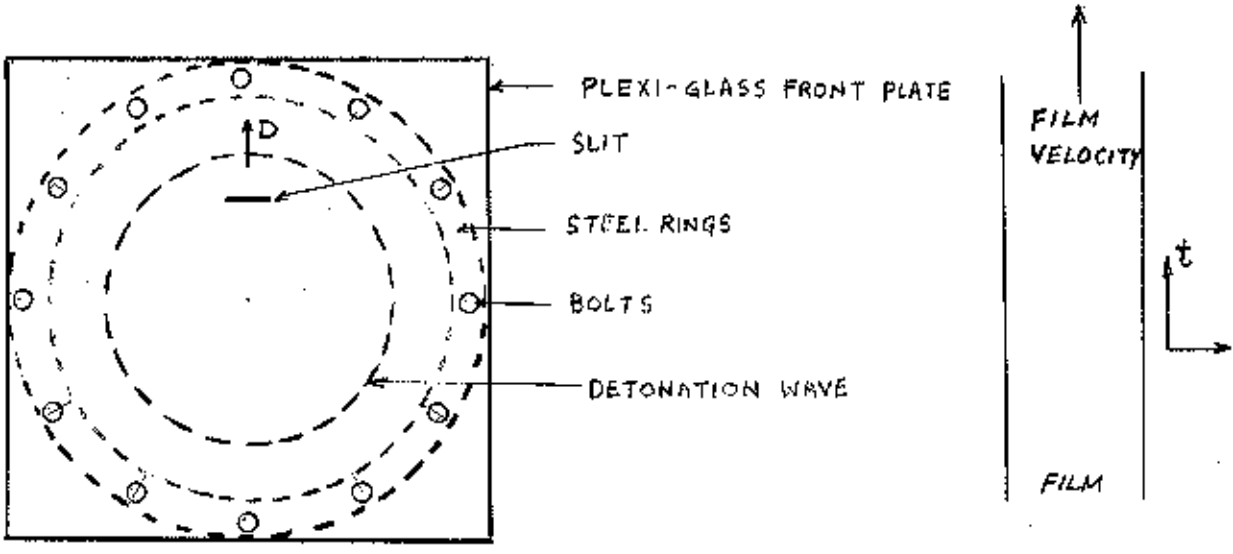

FIGURE 16 ARRANGEMENT FOR TAKING VERTICAL SLIT PHOTOGRAPHS

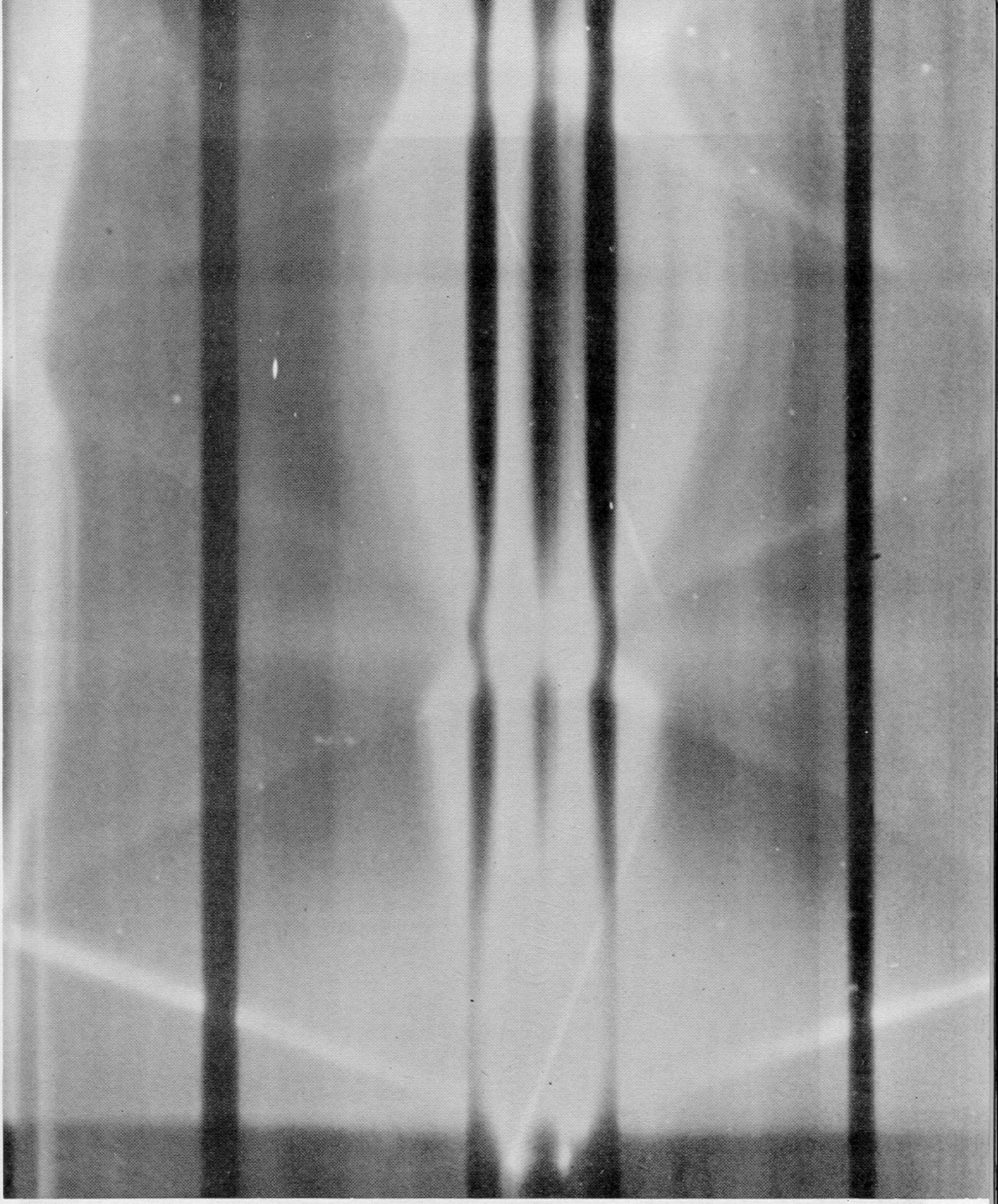

FIG. 17 STREAK PHOTOGRAPH OF CYLINDRICAL DETONATION (INITIATION BY EXPLODING WIRE)

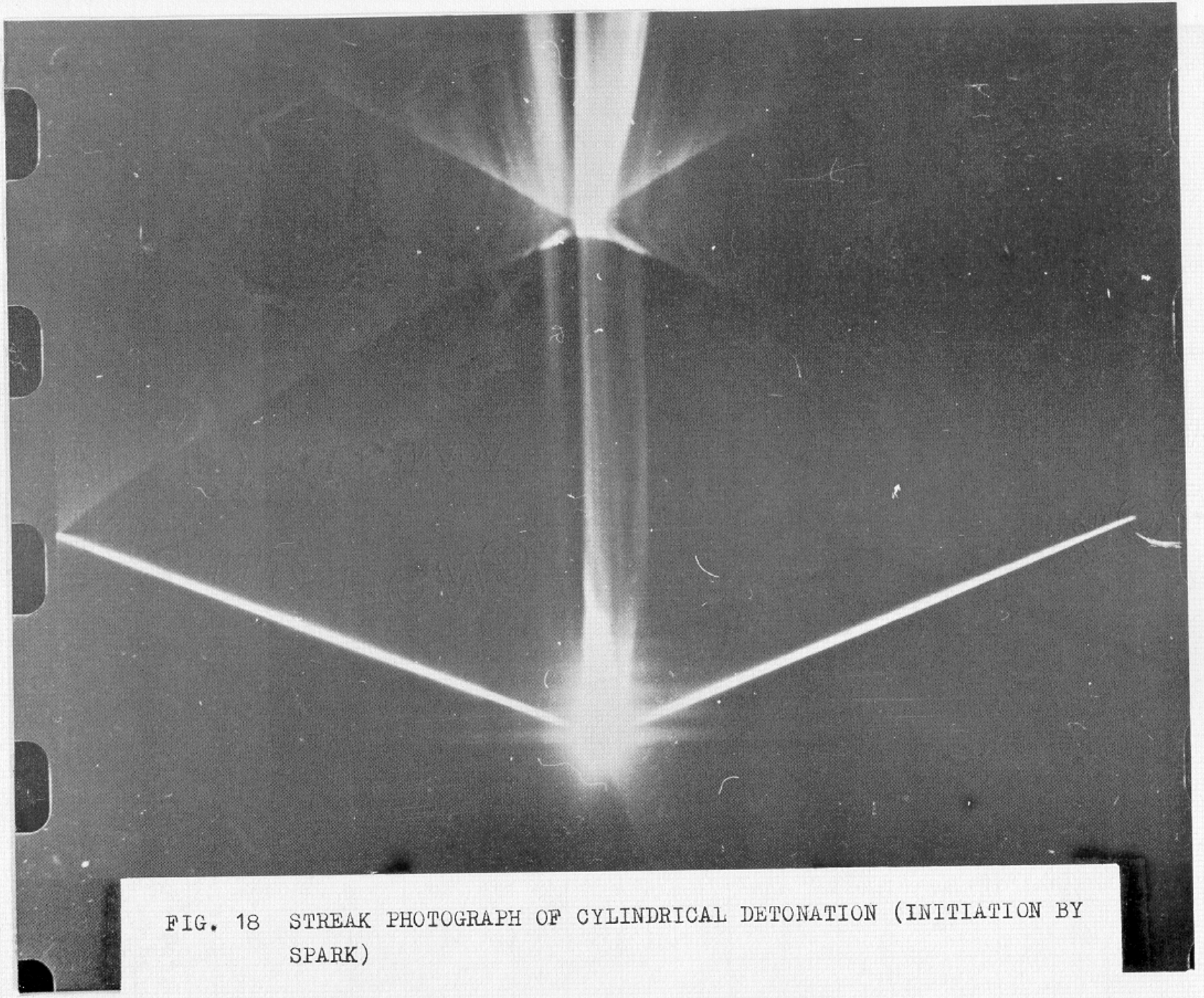

FIG. 18 STREAK PHOTOGRAPH OF CYLINDRICAL DETONATION (INITIATION BY SPARK)

FIG. 19 DETONATION VELOCITIES FOR ACETYLENE-OXYGEN MIXTURES

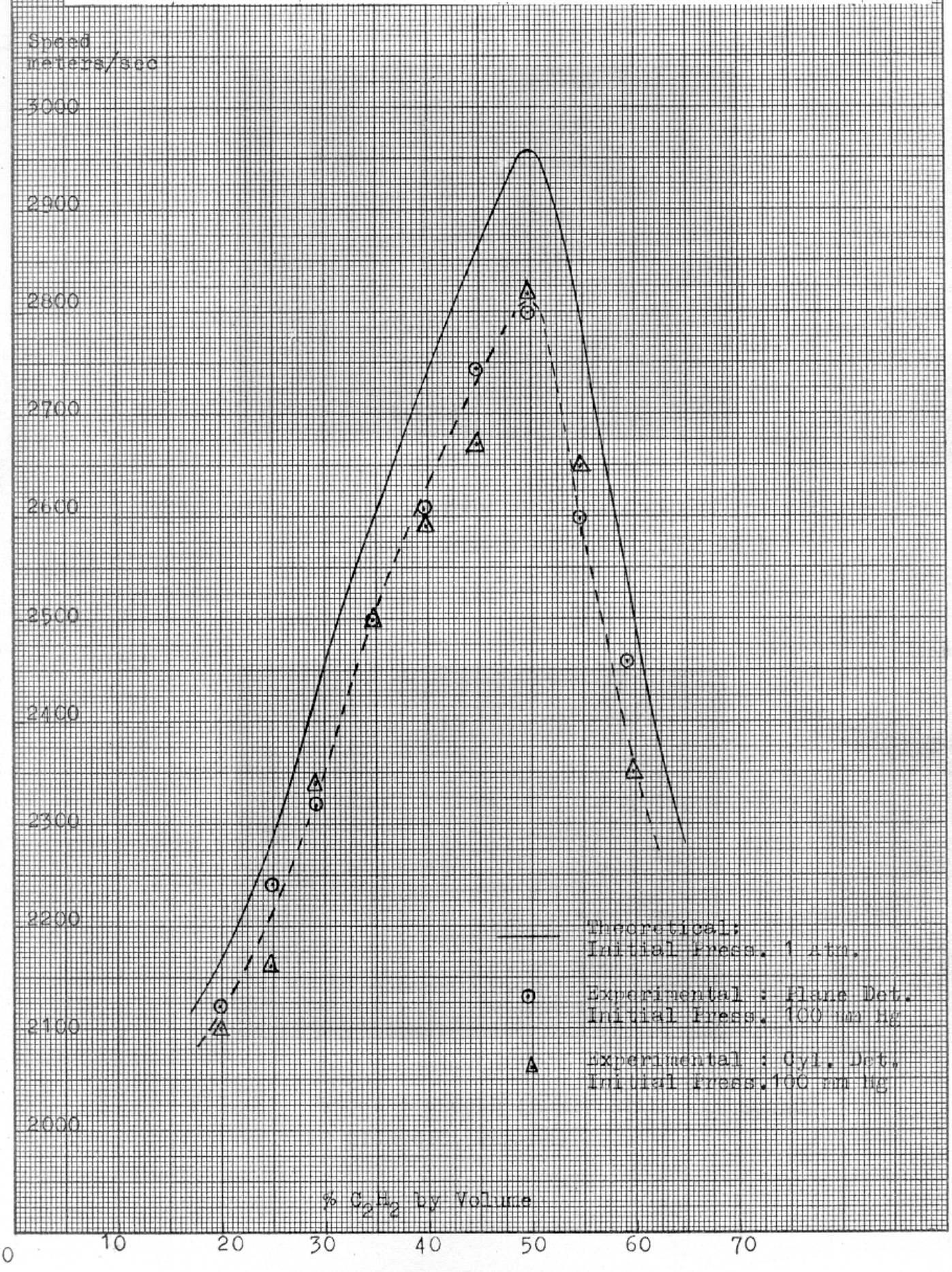

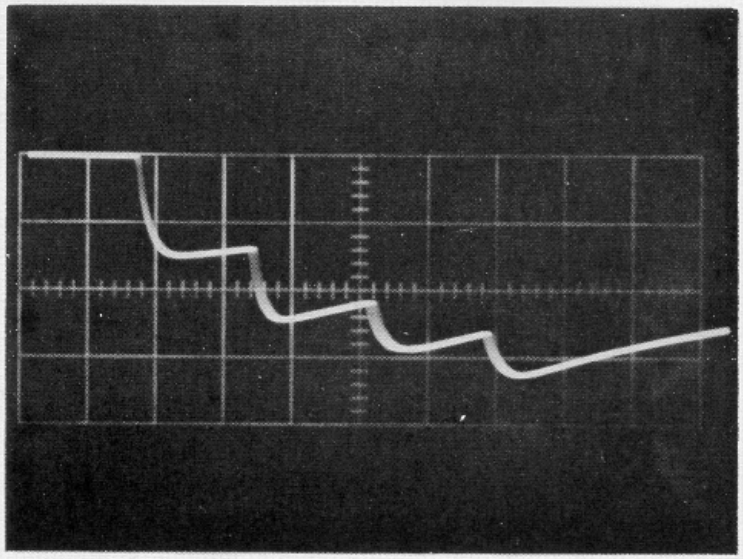

FIG. 20 IONIZATION PROBE RECORD (HORIZONTAL TIME SCALE 5 MICROSEC. PER CM)

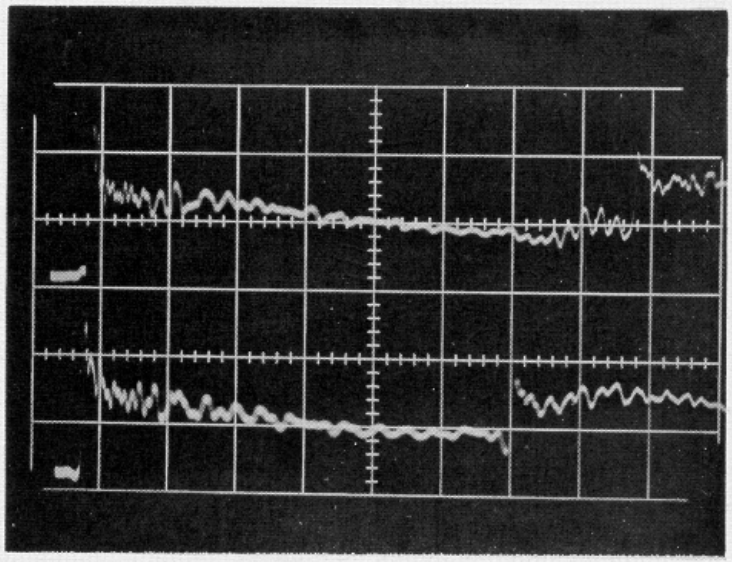

FIG. 21 PRESSURE RECORD (HORIZONTAL TIME SCALE 20 MICROSEC. PER CM)

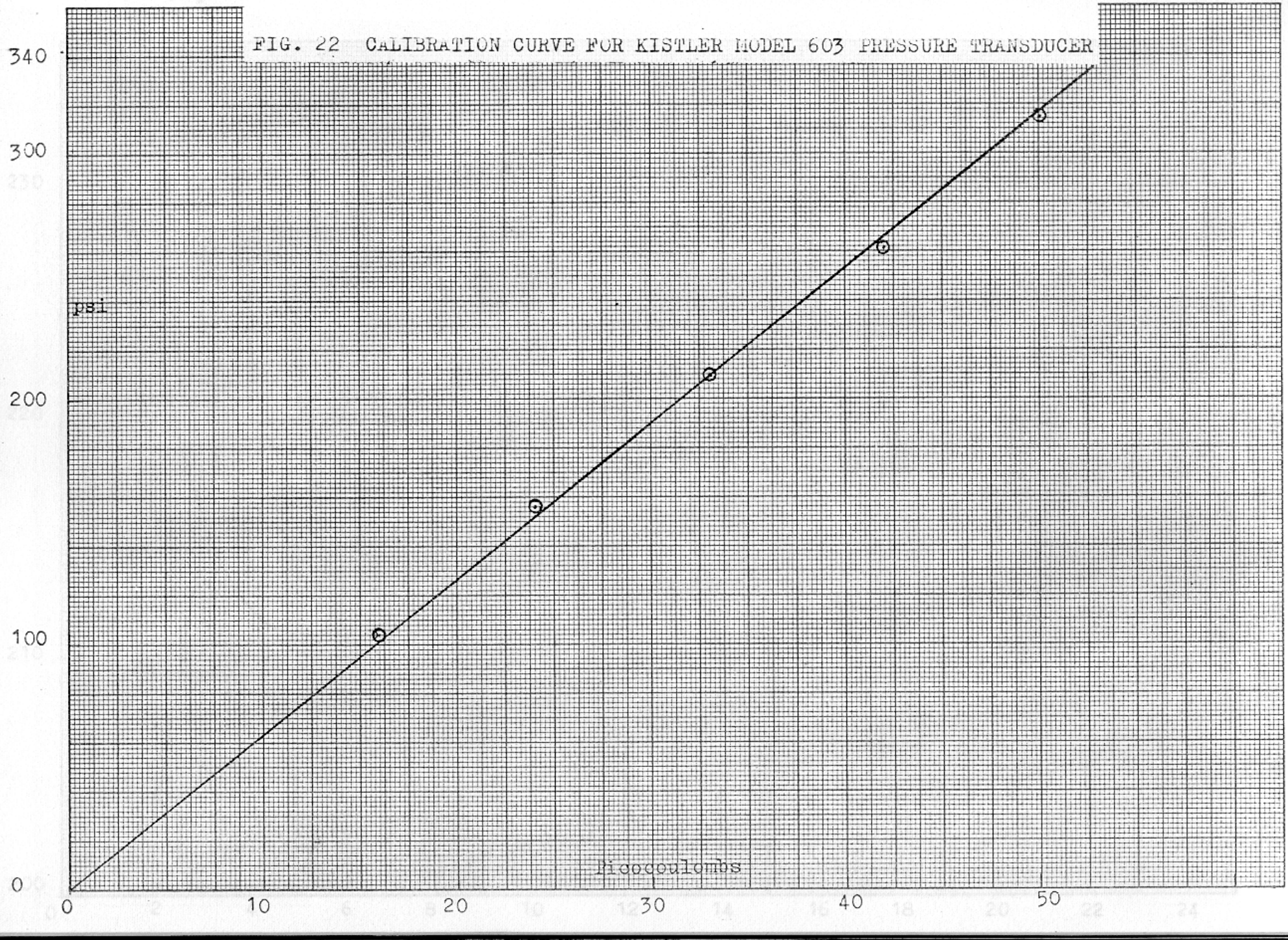
FIG. 22 CALIBRATION CURVE FOR KISTLER MODEL 603 PRESSURE TRANSDUCER
340
300
psi
200
100
0
0
10
20
30
40
50
Picocoulombs

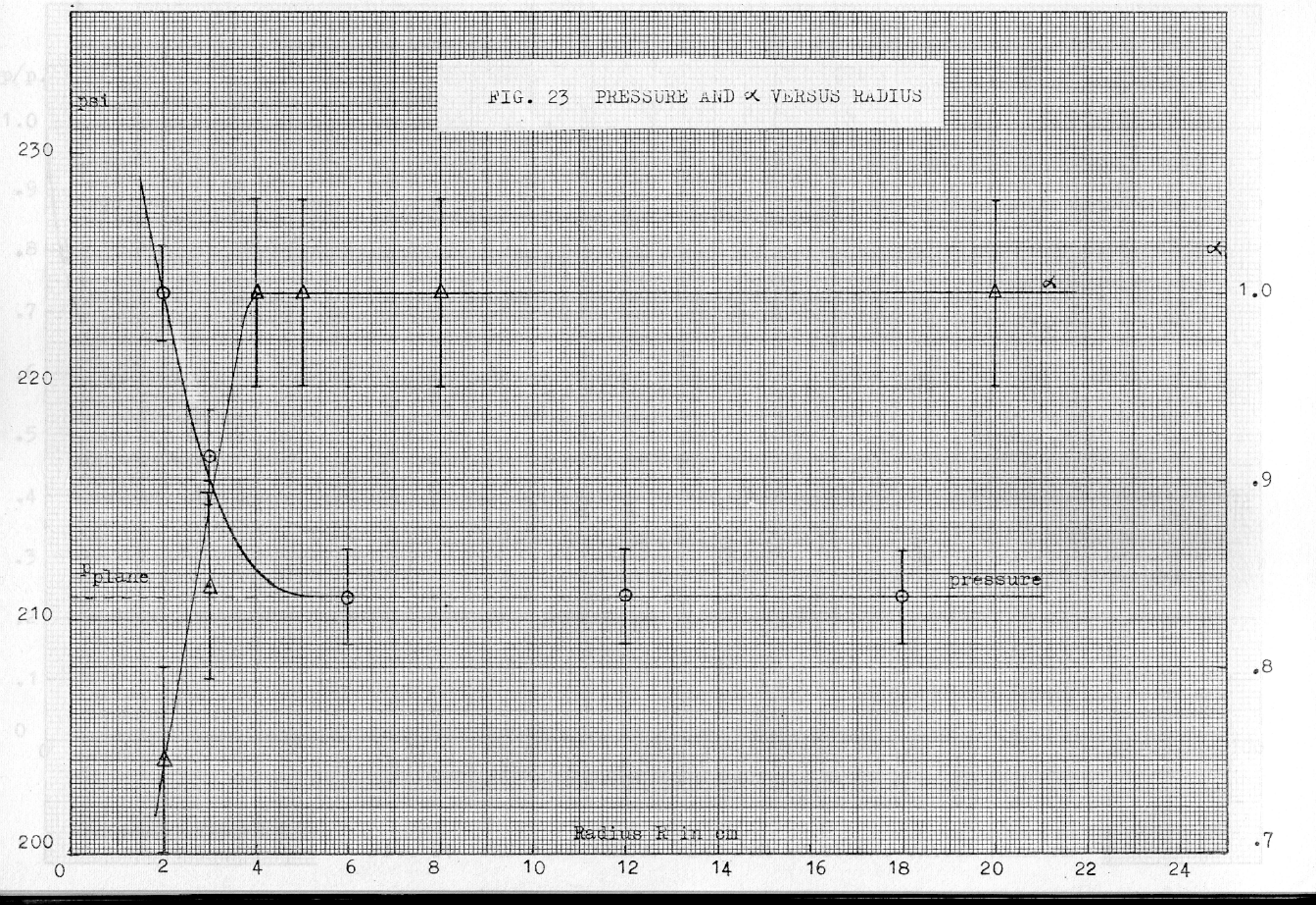
FIG. 23 PRESSURE AND ∝ VERSUS RADIUS
psi
230
220
210
200
P plane
pressure
∝
1.0
.9
.8
.7
Radius R in cm
0
2
4
6
8
10
12
14
16
18
20
22
24

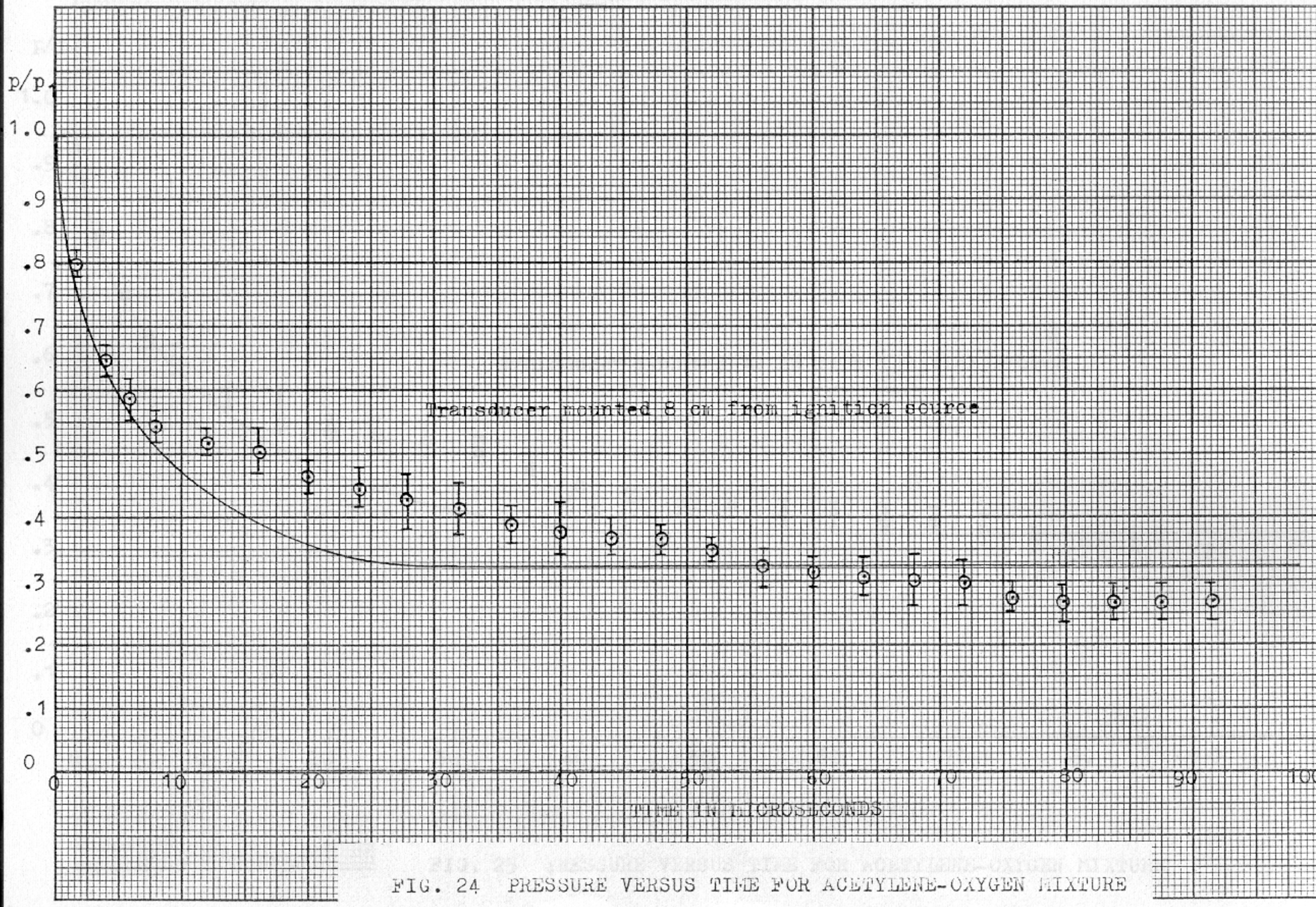

FIG. 24 PRESSURE VERSUS TIME FOR ACETYLENE-OXYGEN MIXTURE

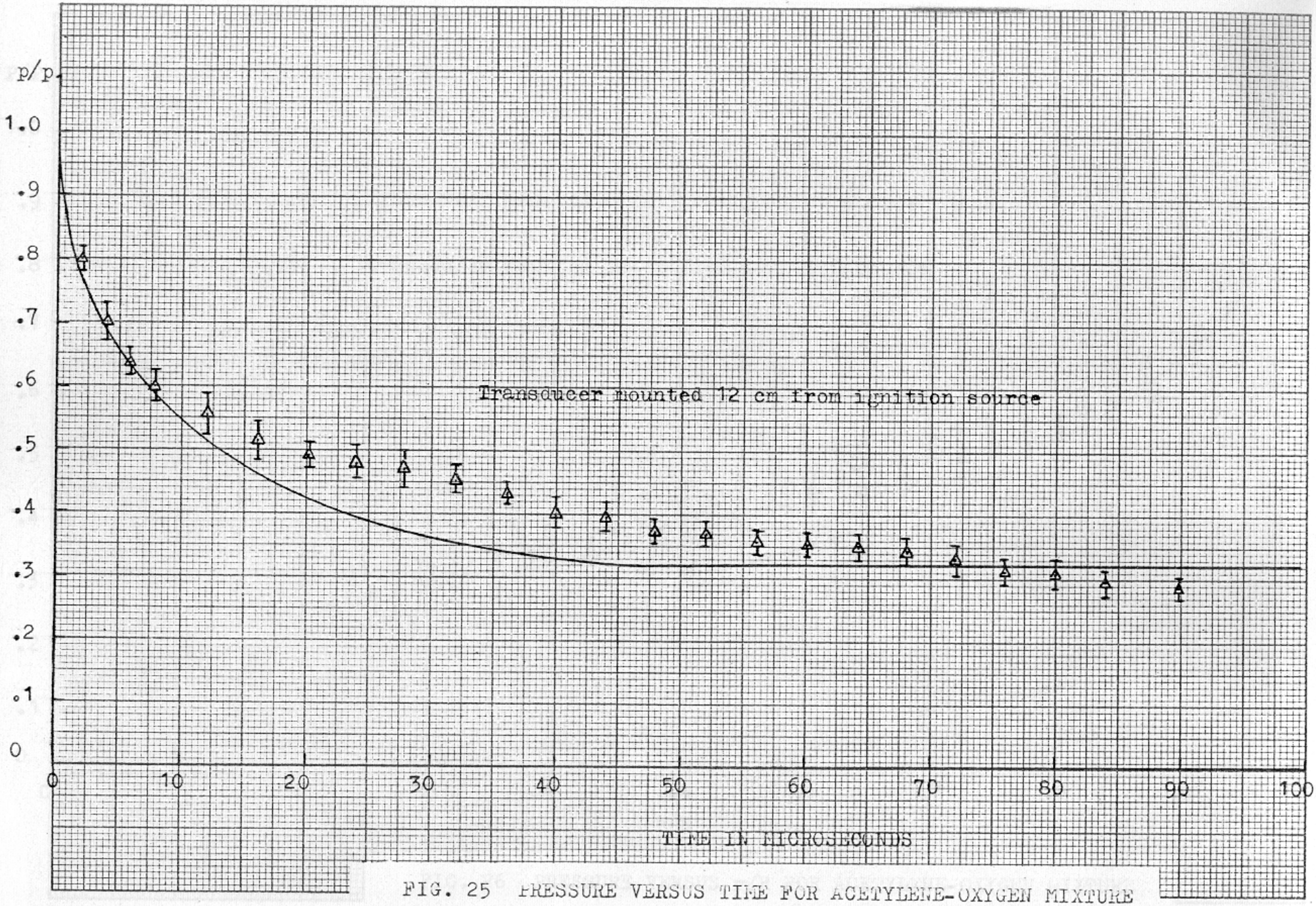

FIG. 25 PRESSURE VERSUS TIME FOR ACETYLENE-OXYGEN MIXTURE

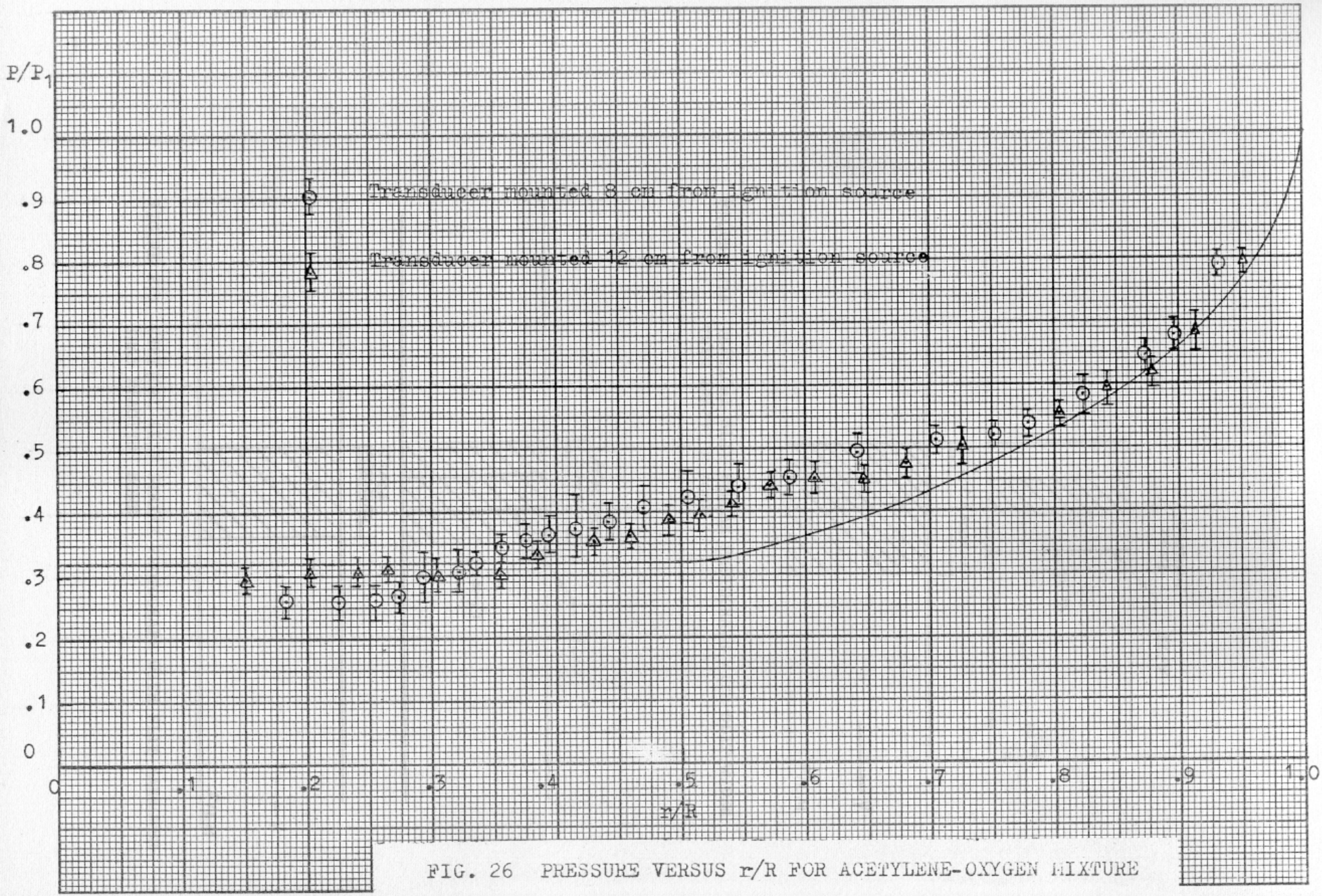

FIG. 26 PRESSURE VERSUS r/R FOR ACETYLENE-OXYGEN MIXTURE

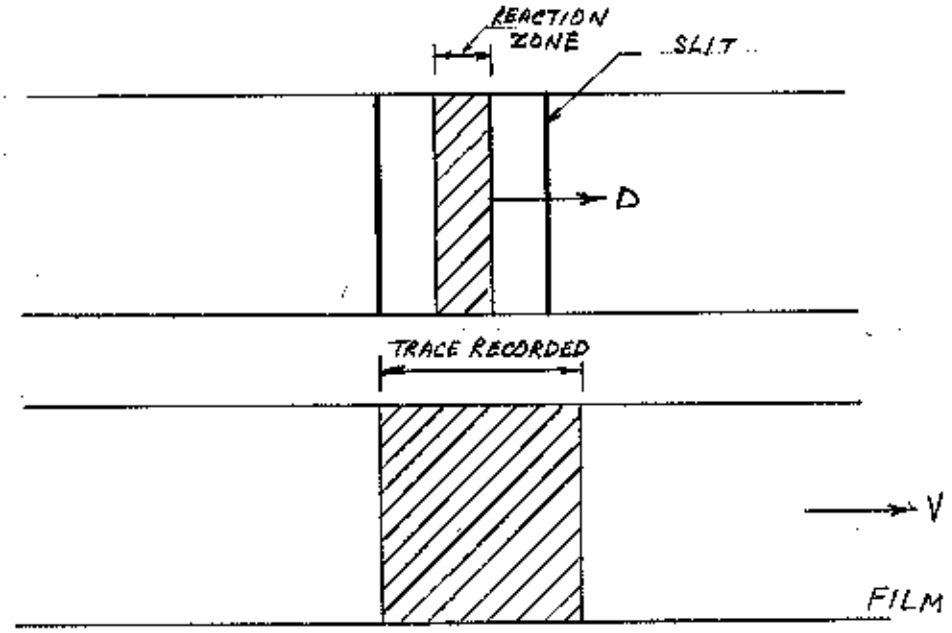

FIGURE 27a VERTICAL SLIT STREAK PHOTOGRAPH WITH SLIT WIDER THAN REACTION ZONE

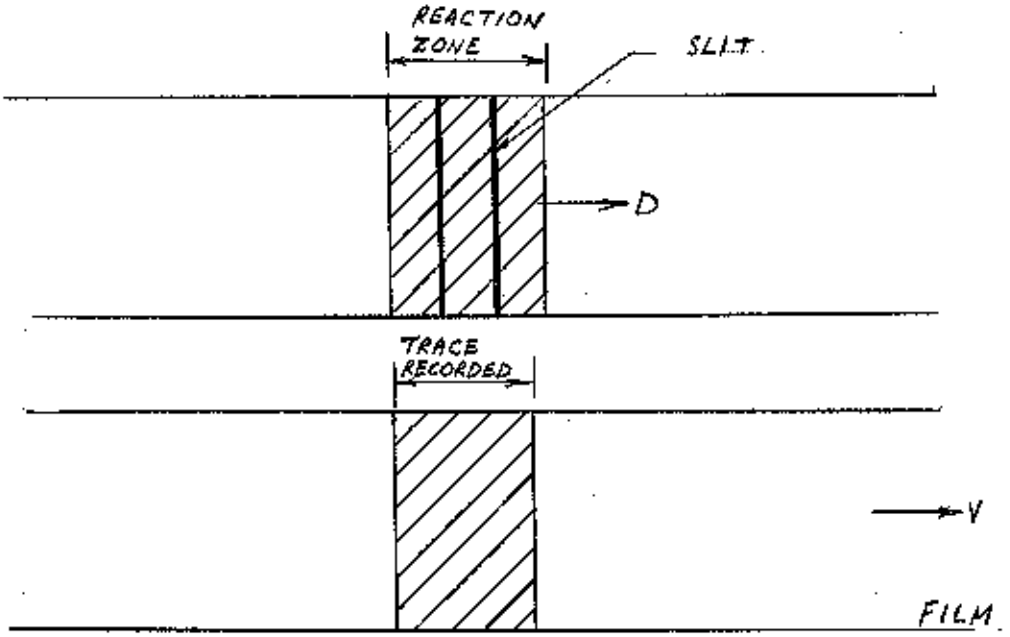

FIGURE 27b VERTICAL SLIT STREAK PHOTOGRAPH WITH SLIT NARROWER THAN REACTION ZONE

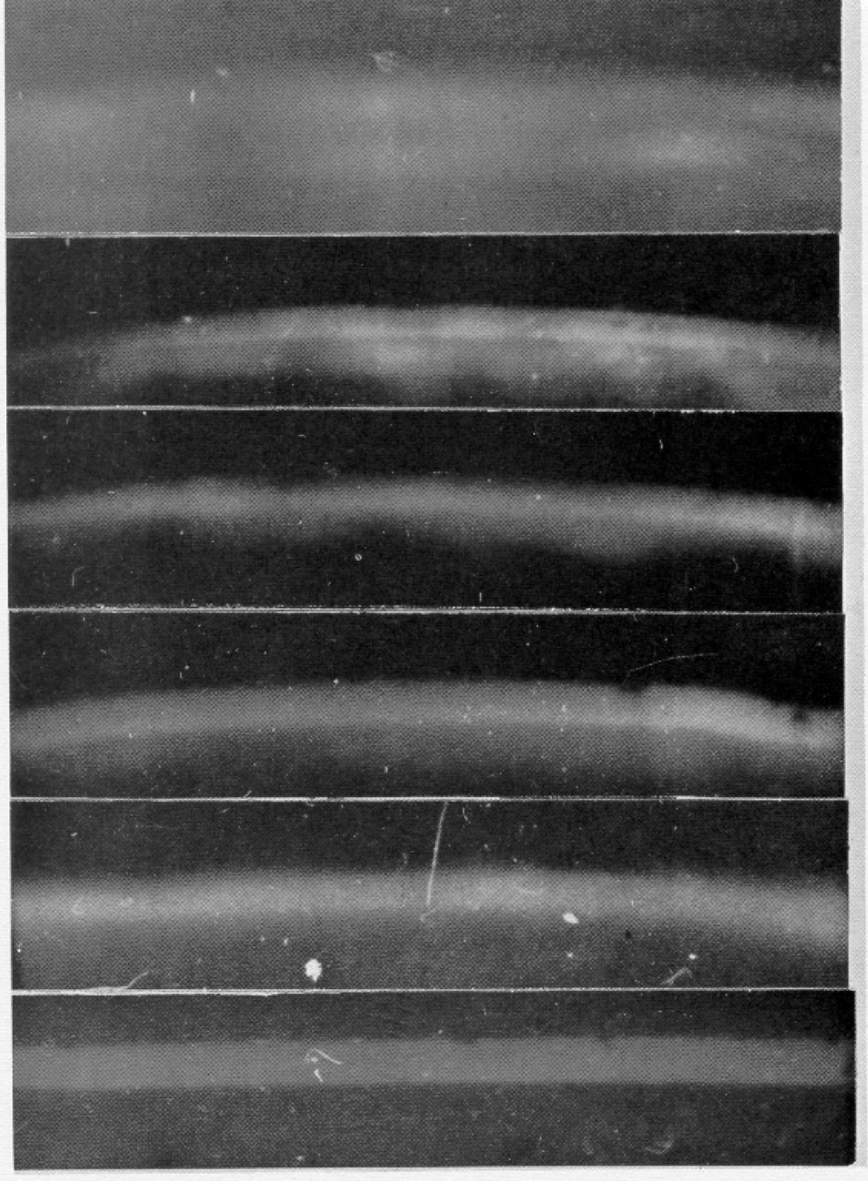

FIG. 28 Vertical Slit Streak Photographs of Cylindrical Detonation Waves

Length of slit = 2 cm.
Width of slit = 1 mm.
Camera speed = 220 rps.
Camera distance= 9 ins.

A. Slit 1 cm. from ignition source
B. Slit 2 cm. from ignition source
C. Slit 3 cm. from ignition source
D. Slit 4 cm. from ignition source
E. Slit 5 cm. from ignition source
F. Slit 8 cm. from ignition source

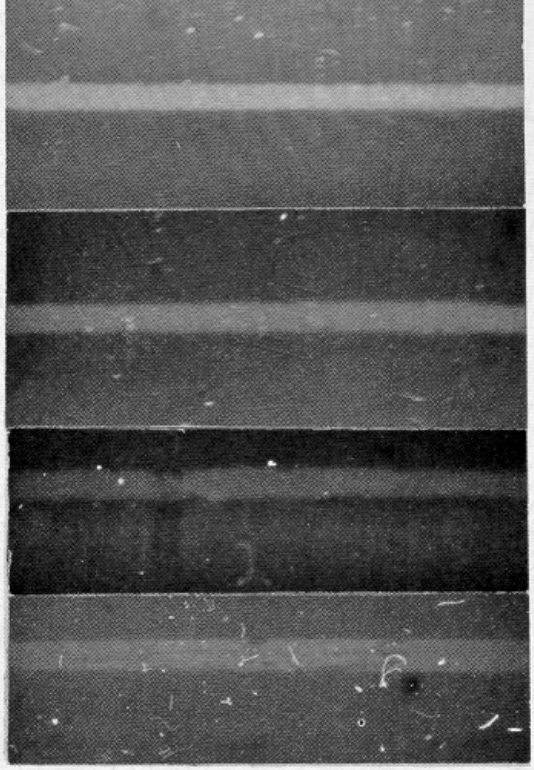

FIG. 29 Vertical Slit Streak Photographs of Cylindrical and Plane Detonation Waves
Length of Slit = 2 cm.
Width of Slit = 1 mm.
Camera Speed = 220 rps
Camera Dist. = 9 ins.

A. Cylindrical Detonation-Slit 3 cm. from ignition source
B. Cylindrical Detonation-Slit 20 cm. from ignition source
C. Plane Detonation-Slit 3 cm. from ignition source
D. Plane Detonation-Slit 20 cm. from ignition source

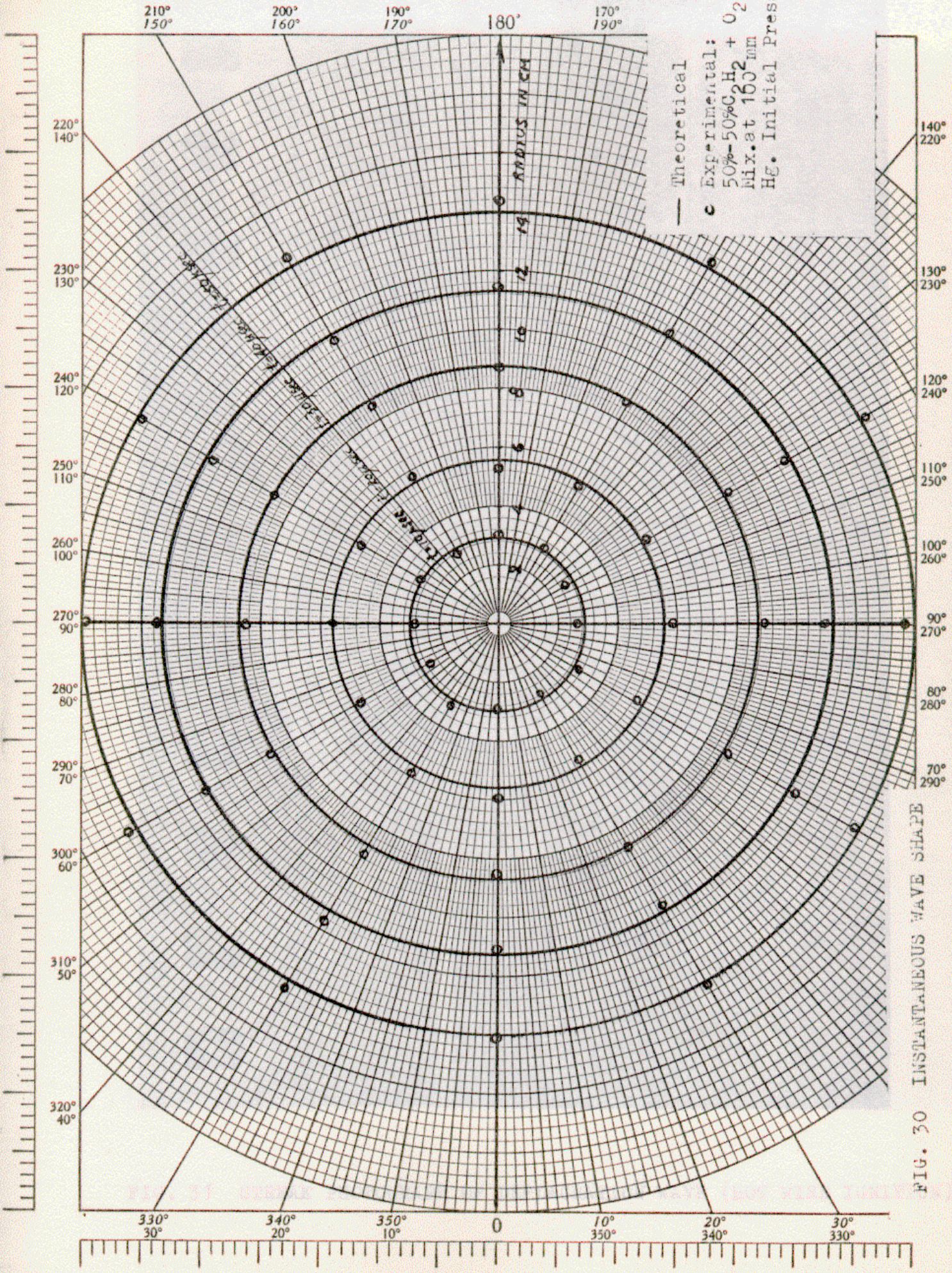

FIG. 30 INSTANTANEOUS WAVE SHAPE

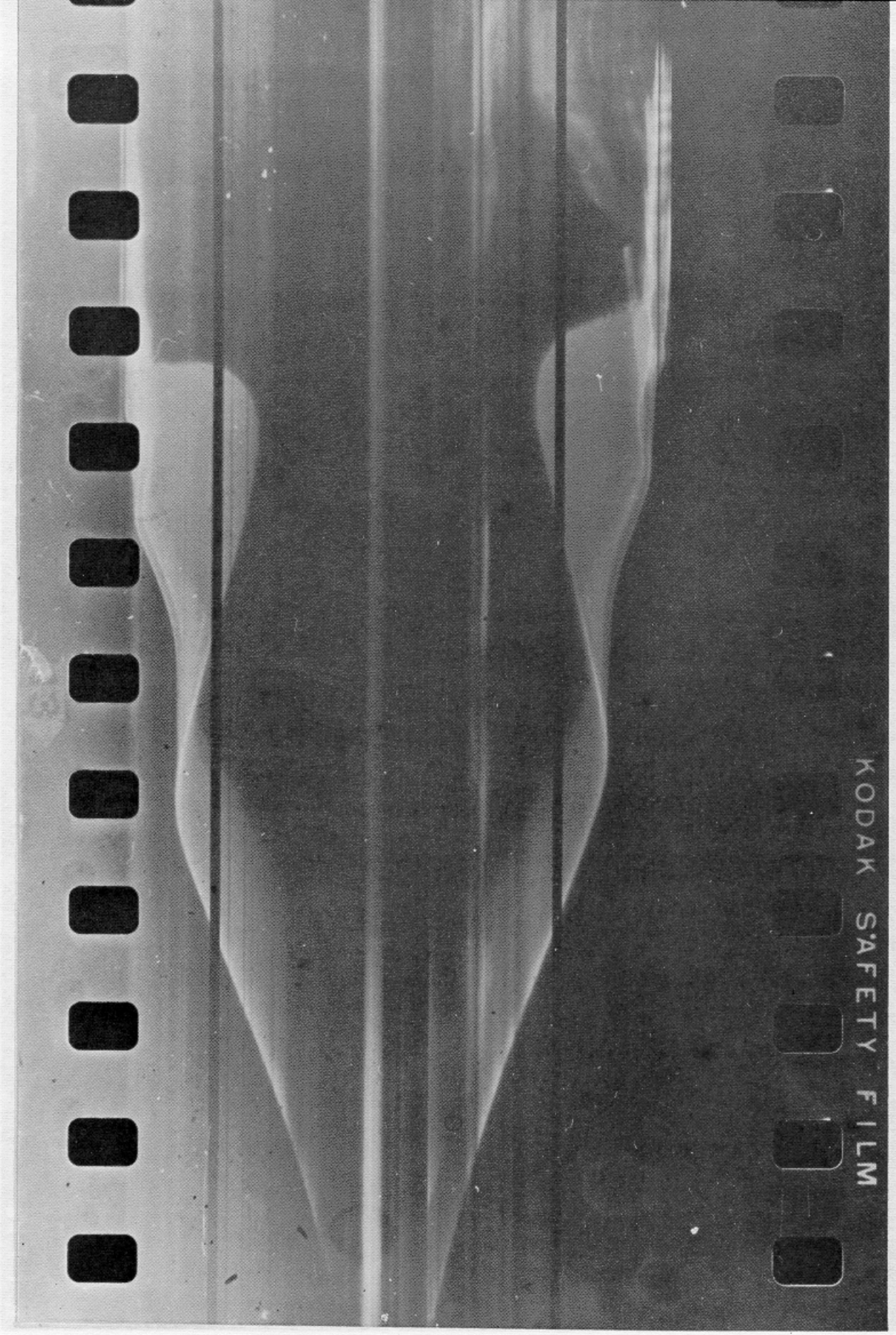

FIG. 31 STREAK PHOTOGRAPH OF DEFLAGRATION WAVE (HOT WIRE IGNITION)

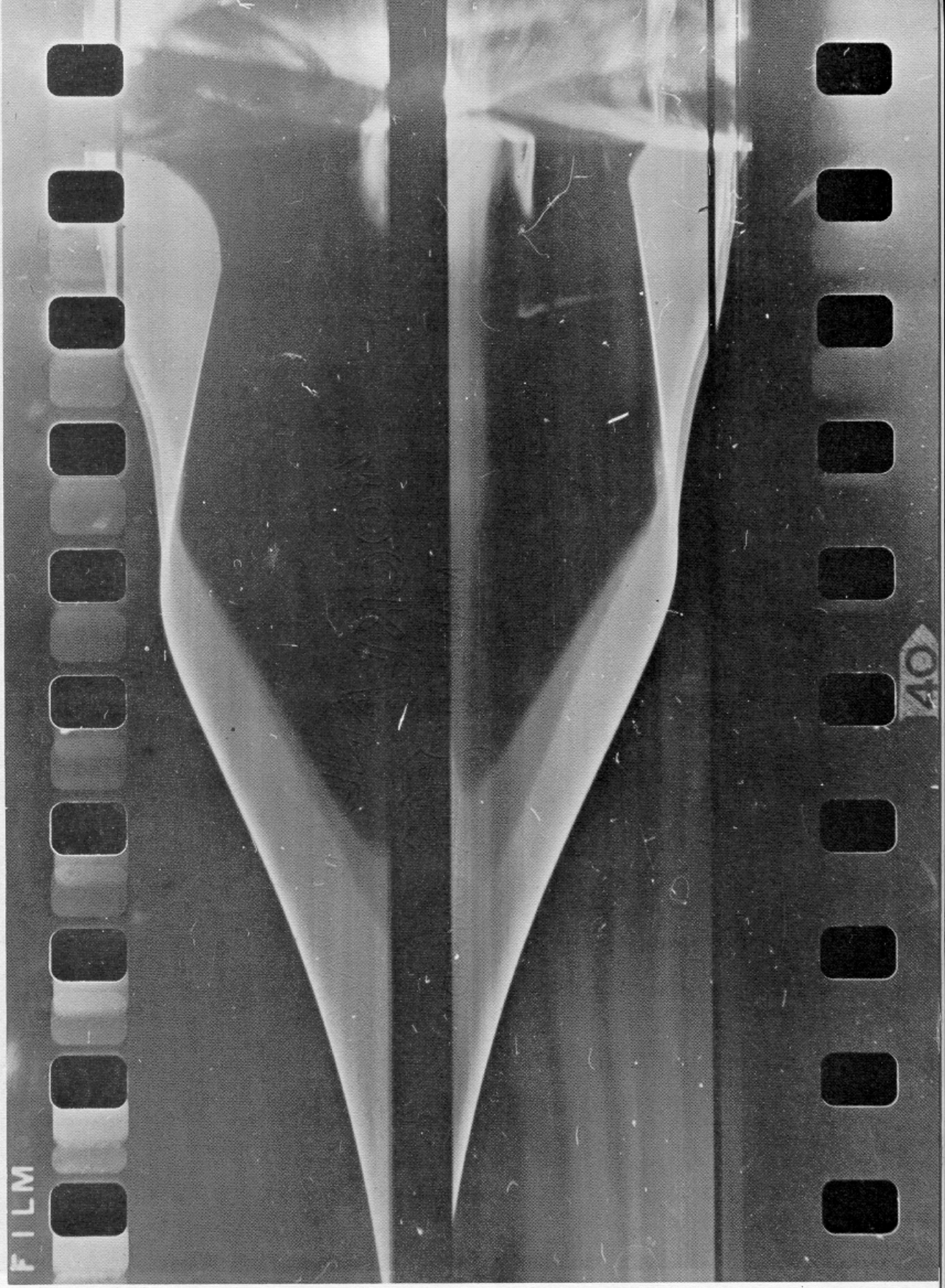

FIG. 32 STREAK PHOTOGRAPH OF DEFLAGRATION WAVE (SPARK IGNITION)

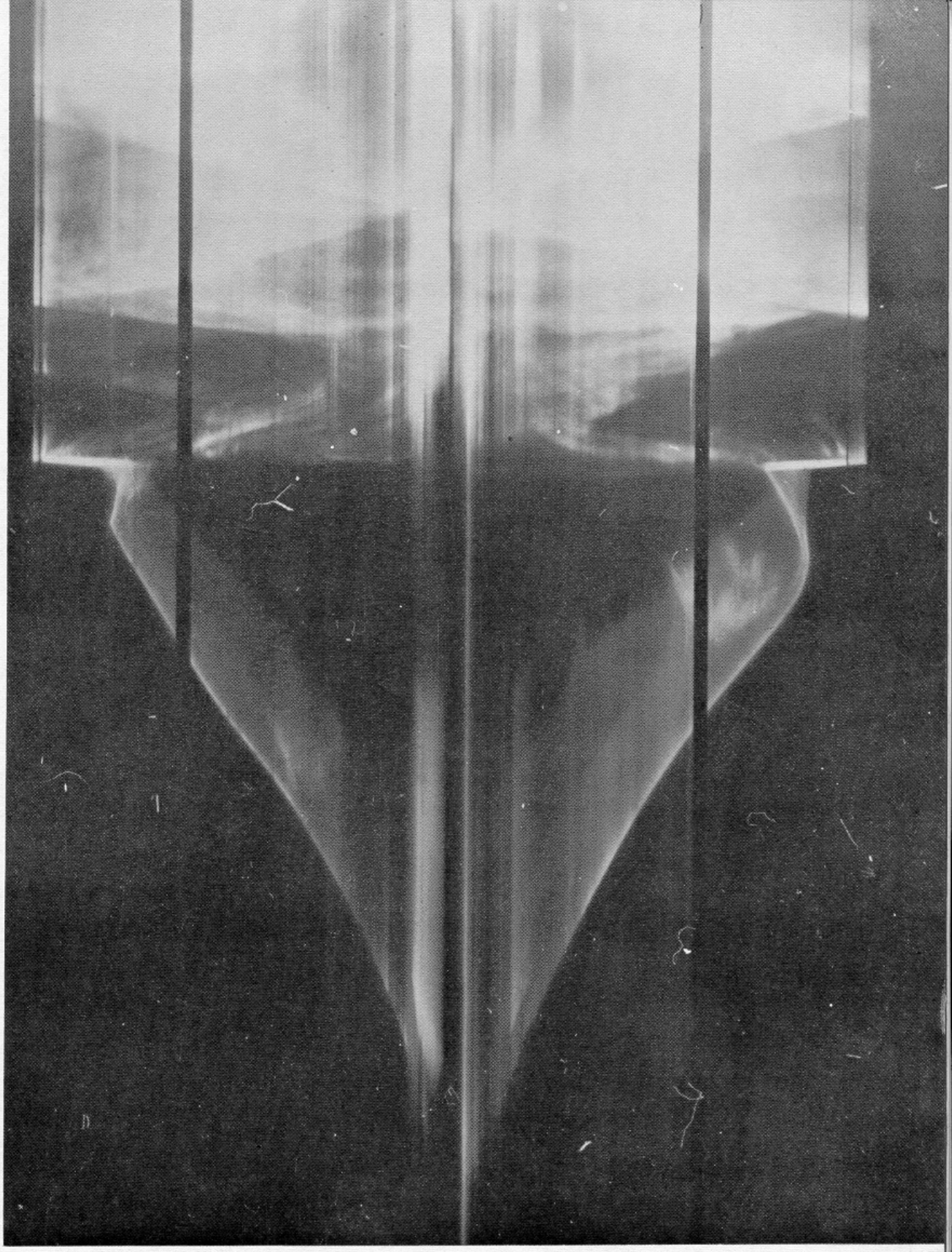

FIG. 33 STREAK PHOTOGRAPH OF DEFLAGRATION WAVE(WITH 1/8" DIA. WIRE SPIRALLED ON ONE FACE OF THE CYLINDRICAL VESSEL-- TRANSITION OBSERVED)